Morse and Drainage Description and Encoding of Images

Vicent Caselles *
Guillermo Sapiro †
Andres Solé ‡

October 18, 2002

Abstract

In this paper we develop and analyze basic geometric structures for the topographic representation of images. One component of the geometric description is based on the Morse structure of the image, while a second one is connected to its drainage structure. These fundamental descriptors could be used as building blocks for a geometric multiscale representation of images in general and Digital Elevation Models (DEM) in particular. The topographic significance of the Morse and drainage structures of DEMs suggests that they can be used as the basis of an efficient encoding scheme. Therefore, we combine this geometric representation with partial differential equations based interpolation algorithms and lossless data compression techniques to develop a compression scheme for DEM. This algorithm permits to obtain compression results while controlling the maximum error in the decoded elevation map, a property that is necessary for the majority of applications dealing with DEM. We present the underlying theory and compression results for standard DEM data.

Mathematics Subject Classification: 68U10, 54C30, 35J25

Key words: Digital elevation images, mathematical morphology, Morse theory, drainage structures, connected components, interpolation, encoding, compression

1 Introduction

A geometric approach for encoding and compressing Digital Elevation Models (DEM) is proposed and studied in this paper. The proposed approach is based on the computation of the singularities of the topographic structure of the data, a kind of topological Morse theory, and the computation of its drainage structures. Together, they lead to an efficient representation of the topographic structures of these images. These basic structures can also be considered as a building block for the geometric multiscale representation of DEM.[1] The emphasis and novelty of this paper is in the mathematics behind this framework, while the applications were reported in [58].

DEM data consist of a discrete digital representation of a surface terrain. Each cell in a DEM corresponds to a point (x, y, z) in 3D space. We can think of (x, y) as the coordinates in the image domain and the height

*Dept. de Tecnologia, Universitat Pompeu-Fabra, Passeig de Circumvalació, 8, 08003 Barcelona, Spain, vicent.caselles@tecn.upf.es

†Department of Electrical and Computer Engineering, University of Minnesota, Minneapolis, MN 55455, USA, guille@ece.umn.edu

‡Dept. de Tecnologia, Universitat Pompeu-Fabra, Passeig de Circumvalació, 8, 08003 Barcelona, Spain, andreu.sole@tecn.upf.es

[1] The explicit combination of the theory developed in this paper with classical multiscale analysis in general and multiscale compression in particular is subject of current work in collaboration with Ron DeVore and results in this direction will be reported elsewhere.

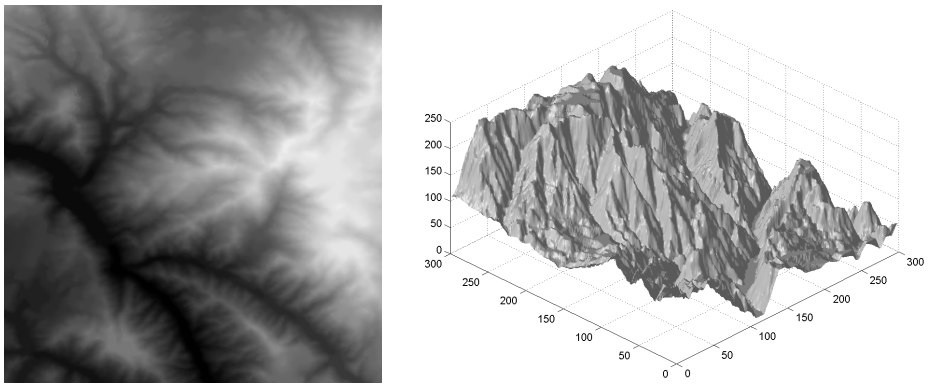

Figure 1: Left: original DEM image. Right: 3D representation of the image on the left.

z as the gray value of the image (see Fig. 1). The acquisition systems used to obtain a DEM have been improved during the last years in order to obtain a better resolution both in the coordinate plane and in height.

Obviously, this kind of data requires a large amount of bytes to store them. Typically a DEM image from a small terrain has 1200×1200 points, that is 1440000 bytes ($1.4Mb$) when using 8 bits for the height, or 2880000 ($2.8Mb$) when using 16 bits. If we note that for a complete terrain description of a country we need thousands of these images, storing and transmitting them requires efficient encoding and compression.

Many algorithms exist for data compression. They can be classified into lossless and lossy [48, 66, 65]. Lossless algorithms introduce no error, thereby limiting the amount of achieved data compression. Lossy algorithms achieve higher compression ratios at the expenses of introducing errors in the decoded image. It is important in this case to have a control on this error. Typically, lossy compression algorithms control the L_2 norm of the error (the root mean square error), but it is not so easy to find algorithms which allow a control on the L_∞ norm of the error (that is the sup error). This is fundamental for DEM applications. Without an L^∞ error control the error in individual pixels may be of the same order of magnitude as the image gray value resolution. For DEM applications, e.g., navigation and landing, this leads to an error in terrain height that makes the algorithm forbidden. A standard algorithm allowing the desired L_∞ control is JPEG Lossless (JPEG-LS) [66, 65, 43], which has a near lossless mode where one can impose the maximum allowed error. The use of JPEG-LS for DEM data has been studied in [43].[2]

As mentioned above, the control of the maximum error per pixel (terrain point) is required when compressing DEM data to achieve an accurate description of terrain features. On the other hand, in the case of DEM data, it seems reasonable to store only those geometric structures which are of special relevance (such as its Morse and drainage structures, see below), and interpolate, while controlling the maximal error, the rest from this non uniform geometric sampling. The goal of this paper is to compute these structures and to use them to efficiently compress DEM data, while controlling the L_∞ norm of the error. The geometric description of the data is based on a kind of topological Morse theory and on drainage structures, which provide, as we will show below, an efficient topographic representation of the image.

This paper is structured as follows. Section 2 reviews the current literature in topographic representation of images and will help us to further motivate our geometric approach for DEM encoding. Section 3 describes the notion of monotone and maximal monotone section. In Section 4 we recall the definition and basic properties of some morphological filters introduced by Luc Vincent which are called the extrema killers. In Section 5 we recall some results about the effect of the extrema killers on images, they simplify

[2]Let us mention that if we compress an image with JPEG-2000 [1] and then encode the errors which are greater than a given bound, then this algorithm can also be used to compress with control of the maximum error.

its topographic map, in particular, the number of maximal monotone sections of an image is always finite if we previously filter it by means of Vincent's filters. Next, in Section 6, we will define the notion of critical and singular value and prove that they are equivalent. As a main consequence, we propose a simple combinatorial algorithm computing the maximal monotone sections of an image. This is the object of Section 6.1. Section 7 will be devoted to the study of *drainage* structures from a morphological point of view. Section 8 is devoted to the computation of the drainage structures. In Section 9 we discuss some properties of the interpolation algorithms used to recover an approximation of the original data from the sampled one. In Section 10 we collect the previously developed algorithms and we apply them to build an algorithm adapted to the compression of DEM data. We also compare it with existing compression algorithms, mainly with JPEG Lossless (JLS) and JPEG-2000. Finally, in Section 12 we summarize the main conclusions of this work.

2 Review on the topographic description of images

The use of a topographic description of images, surfaces, or $3D$ data has been introduced and motivated in different areas of research, including image processing, computer graphics, and geographic information systems (GIS), e.g., [8, 9, 10, 7, 6, 12, 18, 20, 23, 30, 61, 33, 39, 38, 49, 52, 57]. The motivations for such a description differ depending on the field of application. In all cases these aim to achieve an efficient description of the basic shapes in the given image and their topological changes as a function of a physical quantity that depends on the type of data (height in data elevation models, intensity in images, etc.). In our brief literature review below, which will help to motivate our own contribution, we have separated the works into two main areas of research: computer graphics and image processing. In some cases this separation is somewhat arbitrary, some papers, if not all, could be included in both areas, since the application could be oriented to one or the other.

In computer graphics and geographic information systems, topographic maps represent a high level description of the data. Topographic maps are represented by contour maps, i.e., the isocontours of the given scalar data. The description of the varying isocontours requires the introduction of data structures, like the *topographic change tree* or *contour tree* which can represent the nesting of contour lines on a contour map (or a continuous topographic structure) [47, 30, 61]. In all cases, the proposed description can be considered as an implementation of Morse theory, in the sense that Morse theory describes the topological change of the isocontours of scalar data or height function as the height varies, and relates these topological changes to the criticalities of the function. Given the scalar data u defined in a domain Ω of $\mathbb{R}^N$ ($u : \Omega \to \mathbb{R}$), the contour map is defined in the literature as the family of isocontours $[u = \lambda] = \{x \in \Omega : u(x) = \lambda\}$, $\lambda \in \mathbb{R}$, or in terms of the boundaries of upper (or lower) level sets $[u \geq \lambda] = \{x \in \Omega : u(x) \geq \lambda\}$ ($[u \leq \lambda]$). The first description is more adapted to the case of smooth data while the second description can be adapted to more general continuous data where there are plateaus of constant elevation or discontinuous data. The second description has been addressed in [18, 30], while the first description has been used in [7, 6, 61], where an a priori interpolation of the discrete data is required so that the regularity assumptions permit the isocontour description.

The contour map is organized in a data structure, either the contour tree [30, 61], or the Reeb graph [60, 44]. The contour tree represents the nesting of contour lines of the contour map. According to [30], each node represents a connected component of an upper (or lower) level set $[u \geq \lambda]$ ($[u \leq \lambda]$), and links between nodes represent a parent-child relationship, a link going from the containing to the contained set in the upper tree, or viceversa if we consider the lower tree. Each node has a list of descendants, its corresponding elevation value, a list of boundary points, and its parent. The contour tree encodes the topological changes of the level curves of the data. Critical values and its associated features, peaks (maxima), pits (minima), or passes (saddles), can be extracted from the contour tree [30]. The description of the topographic changes

requires the use of both upper and lower trees, and the contour tree can also be used as a tool to compute other terrain features such as ridges and ravines [30]. For practical applications, the data structure has to be implemented with a fast algorithm and with minimal storage requirements. In [61] this is accomplished with a variant of the contour tree where the criticalities (maxima, minima, saddles, computed in a local way) are computed first. In [7] several attributes have been added to the contour data which can be used to select a subsampled family of contours which are representative of the data. As examples of such attributes the authors choose the length or area of the isocontours, the ratio length of the isocontour/area of the enclosed set, or the integral of the gradient along the isocontour.

A related data structure is the *Reeb graph*, which represents the splitting and merging of the isocontours. The *Reeb graph* of the height function u is obtained by identifying two points $p, q \in \Omega$ such that $u(p) = u(q)$ if they are in the same connected component of the isocontour $[u = u(p)]$. Thus, a cross-sectional contour corresponds to a point of an edge of the Reeb graph, and a vertex represents a critical point of the height function u. The Reeb graph was proposed in [60] as a data structure for encoding topographic maps. The authors proposed to compute it following the computation of the so-called surface network. The surface network is also a topological graph, i.e., a graph that represents the relations among critical points, whose vertex are critical points and the edges represent either a ridge or a ravine line. A ridge (ravine) line is a line with steepest gradient which joins a pass to a peak (pit) [60, 26]. The critical points are computed with an algorithm based on local computations, so that the Euler's formula relating the number of peaks, pits and passes, holds. Then ridges and ravines are computed following the steepest lines. In the context of computer graphics, Morse theory has also been used to encode surfaces in $3D$ space [57]. In [57], the authors also use a tree structure like the Reeb graph complemented with information about the Morse indexes of the singularities and including enough (information about) intermediate contours to be able to reconstruct by interpolation the precise way in which the surface is embedded in $3D$ space.

In image processing, the topographic description was advocated as a local and contrast invariant description of images (i.e., invariant under illumination changes), and has lead to an underlying notion of shapes of an image as the family of connected components of upper or lower level sets of the image [12, 49, 52, 13]. An efficient description of the family of shapes in terms of a tree was proposed in [39, 38] and further developed in [33]. The tree of shapes as proposed in [39, 38] fuses the information of both the trees of upper $[u \geq \lambda]$ and lower $[u \leq \lambda]$ level sets of the scalar image u. The key idea for this fusion is the notion of shape as a connected component of an upper $[u \geq \lambda]$ or lower $[u < \lambda]$ level set in which the holes are filled-in. This topographic structure has been further studied in [9, 38, 8], where a Morse description of this topographic structure was developed. The mathematical description permitted to include the case of images as upper semicontinuous functions. In [33], following bilinear interpolation of the discrete data, the image could be treated as a continuous function and a tree of bilinear level lines $[u = \lambda]$ was computed. The tree of bilinear level lines is more related to the contour tree computed with the isocontours of the interpolated image. A subtree containing the so-called meaningful level lines [19] can be extracted which contains the main level lines according to the distribution of gradient values of the image in a statistical way [33, 19]. The work in [28] can be considered as a mathematical description of the (iso) contour tree in the case of two-dimensional functions. In [18], Morse theory has also been used as a basic model to describe the geometric structures of $2D$ and $3D$ images, and in general, of multidimensional data. Applications have been given in different domains, in particular, to visualize structures in $3D$ medical images. The data are typically multi-dimensional sampled data, and it cannot be assumed that the function is Morse in a traditional sense, even if interpolated. Thus, the authors adapt Morse theory using combinatorial methods. The authors assume that the given data are interpolated by a continuous real valued functions u. The basic geometric objects studied are the boundaries of the connected components of upper level sets $[u \geq \lambda]$ of u and their variation with the level λ. In their set of axioms, the authors assume that those boundaries are compact, oriented manifolds in $\mathbb{R}^N$, they precise their local structure, and its connection with the original sampled

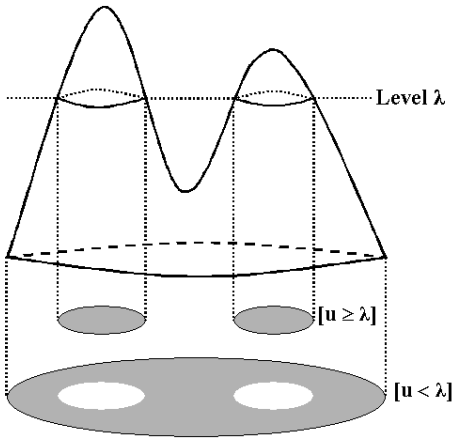

Figure 2: A function u and its upper and lower level sets.

data. In particular, those axioms imply that the topological structure of the sampled data is reflected by any interpolating function satisfying their axioms. Then critical points and critical values are defined, obtaining maximum, minimum, and saddle critical points (and values). Criticalities are defined by local analysis of the function, including the case of degenerate sets (i.e., connected regions of the sampled data with the same values). The authors prove that the topology of their basic objects changes at a critical level, and does not change between critical levels. Then the criticality graph is defined, the vertices of the graph are the criticalities and the edges go between criticalities in such a way that no further criticalities are located between them. The regions represented by each edge are called zones of the critical point with higher value. In each zone the boundaries of the upper level sets are homeomorphic [18]. The topology change at a critical value is computed by combinatorial methods if the critical value is a saddle or a minimum, and by the genus in the case of a maximum value. In some sense, this structure is related to a Reeb graph. Efficient algorithms are proposed which compute the criticality graph [18].

Let us finally mention that a morphological approach to image compression has been proposed by several authors, for instance [42], [41], [51], [45], [21]. In [42],[51] the authors propose to use binary partition trees to select the level curves which have to be encoded. The trees take into account the cost in bits to encode the selected level boundaries and the approximation error (measured with an L^2 norm). In [21], the author selected the level lines taking into account its perceptual significance which was measured in terms of the number of T and X junctions contained in it. Because of our application to the encoding of DEM data, we use a description more adapted to the topographic features of this kind of data.

3 Monotone sections

In this section we will introduce the notions of monotone and maximal monotone sections which are the ones containing no topological changes of the topographic structure.

Let D be a subset of $\mathbb{R}^N$. Given a function $u : D \to \mathbb{R}$, we call upper (lower) level set of u any set of the form $[u \geq \lambda] := \{x \in D : u(x) \geq \lambda\}$ or $[u > \lambda] := \{x \in D : u(x) > \lambda\}$ ($[u \leq \lambda] := \{x \in D : u(x) \leq \lambda\}$ or $[u < \lambda] := \{x \in D : u(x) < \lambda\}$) where $\lambda \in \mathbb{R}$. Figure 2 depicts a function $u : D \subset \mathbb{R}^2 \to \mathbb{R}$ (top) which is thresholded at level $\lambda \in \mathbb{R}$. We see the connected components corresponding to the upper level set ($[u \geq \lambda]$) and the lower level set ($[u < \lambda]$), respectively.

The (upper) topographic map of a function u is the family of the connected components of the level sets of u, $[u \geq \lambda]$, $\lambda \in \mathbb{R}$, the connected components being understood in the relative topology of D. It was

proved in [12] that the topographic map is the structure of the image which is invariant under local contrast changes, a notion also defined in [12]. In [8, 9] the authors studied the Morse structure of the topographic map for continuous functions (a similar study can be done for bounded upper semicontinuous functions). They defined a notion of nonsingular region of the topographic map trying to express the fact that the level lines of the topographic map in a nonsingular region are homotopic, as it happens for smooth functions where singularities are understood in the usual way [37]. A first version of this notion appeared in [13]. Our purpose is to review in some detail some results of [8].

Let $u : D \to I\!R$ be a function. For each $\lambda, \mu \in I\!R$, $\lambda \leq \mu$ we define

$$U_{\lambda,\mu} = [\lambda \leq u \leq \mu] = \{x \in D : \lambda \leq u(x) \leq \mu\}$$

The connected components of a set $X \subseteq I\!R^N$ will be denoted by $\mathcal{CC}(X)$. If $x \in X$, the connected component of X containing x will be denoted by $\mathcal{CC}(X, x)$.

Definition 1 *Let $u : D \to I\!R$ be a continuous function. A monotone section of the topographic map of u is a set of the form*

$$X_{\lambda,\mu} \in \mathcal{CC}([\lambda \leq u \leq \mu]), \tag{1}$$

for some $\lambda, \mu \in I\!R$ with $\lambda \leq \mu$, such that for any $\lambda', \mu' \in [\lambda, \mu]$, $\lambda' \leq \mu'$, the set

$$\{x \in X_{\lambda,\mu} : \lambda' \leq u(x) \leq \mu'\}$$

is a connected component of $[\lambda' \leq u \leq \mu']$.

Proposition 1 *Assume that D is compact. Let $u : D \to I\!R$ be a continuous function such that for each $\lambda, \mu \in I\!R$ with $\lambda \leq \mu$ the set $[\lambda \leq u \leq \mu]$ has a finite number of connected components. Let $\lambda < \mu$, $X \in \mathcal{CC}([\lambda \leq u \leq \mu])$. Then X is a monotone section if and only if for any $\alpha \in [\lambda, \mu]$, $X \cap [u = \alpha]$ is a connected set.*

Proof: Obviously, if X is a monotone section, then for any $\alpha \in [\lambda, \mu]$, the set $X \cap [u = \alpha]$ is connected. To prove the converse statement, suppose that X is not a monotone section. Then there are values $\lambda \leq \alpha \leq \beta \leq \mu$ such that $X \cap [\alpha \leq u \leq \beta]$ is not connected. Observe that $X \cap [\alpha \leq u \leq \beta] \neq \emptyset$ because $\emptyset$ is connected. Let $c = \frac{\alpha+\beta}{2}$. Since $X \cap [\alpha \leq u \leq \beta] = (X \cap [\alpha \leq u \leq c]) \cup (X \cap [c \leq u \leq \beta])$ and $(X \cap [\alpha \leq u \leq c]) \cap (X \cap [c \leq u \leq \beta]) \neq \emptyset$, we conclude that either $X \cap [\alpha \leq u \leq c]$ or $X \cap [c \leq u \leq \beta]$, or both, cannot be connected (since the union of intersecting connected sets is also connected). Let us choose one of the above non connected sets and denote it by $X \cap [\alpha_1 \leq u \leq \beta_1]$. Proceeding iteratively in this way we find a decreasing sequence of intervals $[\alpha_n, \beta_n]$ such that $\cap_n [\alpha_n, \beta_n] = \{\gamma\}$ and $X \cap [\alpha_n \leq u \leq \beta_n]$ are not connected. Now, observe that for all $Y_n \in \mathcal{CC}(X \cap [\alpha_n \leq u \leq \beta_n])$ there exists $Y_{n-1} \in \mathcal{CC}(X \cap [\alpha_{n-1} \leq u \leq \beta_{n-1}])$ so that $Y_n \subseteq Y_{n-1}$. Thus, there are at least two different decreasing sequences of continua (compact connected sets) contained in $X \cap [\alpha_n \leq u \leq \beta_n]$. Since the intersection of a decreasing sequence of continua is a continuum, we conclude that $X \cap [u = \gamma] = \cap_n (X \cap [\alpha_n \leq u \leq \beta_n])$ is not connected. This contradiction proves the proposition. □

The following result, which was proved in [8], permits us to define a monotone section which is maximal with respect to inclusion. Those sets are the non singular sets we mentioned above.

Proposition 2 *Assume that $u : D \to I\!R$ is a continuous function such that for each $\lambda, \mu \in I\!R$ with $\lambda \leq \mu$ the set $U_{\lambda,\mu}$ has a finite number of connected components. Let $\lambda_1, \lambda_2, \mu_1, \mu_2 \in I\!R$. Then, if $X_{\lambda_1,\lambda_2}, X_{\mu_1,\mu_2}$ are monotone sections such that $X_{\lambda_1,\lambda_2} \cap X_{\mu_1,\mu_2} \neq \emptyset$, then $X_{\lambda_1,\lambda_2} \cup X_{\mu_1,\mu_2}$ is also a monotone section. In other words, the union of intersecting monotone sections is a monotone section.*

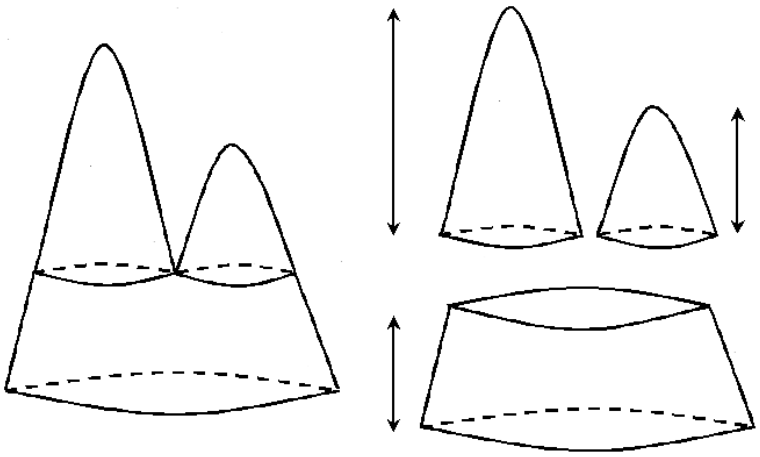

Figure 3: A function u (left) and its decomposition in maximal monotone sections (right).

Let $x \in D$ and $\lambda = u(x)$. For each $\eta \geq \lambda$, let $X_{\lambda,\eta} = \mathcal{CC}(U_{\lambda,\eta}, x)$. We define

$$\eta_+(x,\lambda) = \sup\{\eta : \eta \geq \lambda \quad \text{s. t. } X_{\lambda,\eta} \text{ is a monotone section}\}.$$

Similarly, we define

$$\eta_-(x,\lambda) = \inf\{\eta : \eta \leq \lambda \quad \text{s. t. } X_{\eta,\lambda} \text{ is a monotone section}\}.$$

Note that both numbers are well defined since $X_{\lambda,\lambda}$ is always a monotone section. Note that, by definition, $\eta_-(x,\lambda) \leq \eta_+(x,\lambda)$. By Proposition 2, we may define the (open, closed, half-open, half-closed) interval $I(x,\lambda)$ containing λ whose end-points are $\eta_-(x,\lambda), \eta_+(x,\lambda)$ and which determines a *monotone section containing x maximal with respect to inclusion*, which we denote by $X_{I(x,\lambda)}$. Note that $\lambda \in I(x,\lambda)$ for all $\lambda \in (-\infty, \sup_D u(x)]$. Both functions, $\eta_+(x,\lambda), \eta_-(x,\lambda)$, are nondecreasing functions of λ and have some precise behavior. We shall not give here a detailed description of them. Our purpose will be to prove that, if D is topologically like a ball, $u \in C(\overline{D})$, and there exist some $\delta > 0$ such that $|X| \geq \delta$ for any connected component X of an upper or lower level set, then there is only a finite number of maximal monotone sections in the topographic map of u.

Figure 3 illustrates the notion of maximal monotone section. On the left side we show the original function and on the right side its decomposition on maximal monotone sections.

Remark 1 The notions on maximal monotone sections given in [8] and [9] are based on different approaches. The notion used here is the same as the one used in [8]. The notion used in [9] is adapted to describe the Morse theory of the tree of shapes of the image. It turns out that both notions are equivalent [15].

4 Vincent-Serra filters

The aim of this section is to recall the notion of extrema killer, some morphological filters introduced by L. Vincent, and how these filters simplify the topographic structure of a function. As we shall review in the next section, a function which has been simplified by means of L. Vincent filters will contain a finite number of maximal monotone sections. The results in this section were proved in [8, 14]. Some of them are included in some detail because they will be used below.

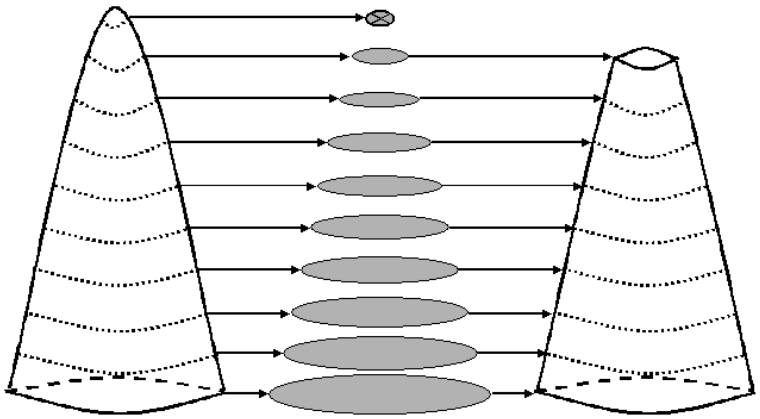

Figure 4: From left to right, the original function u, some of the connected components of $[u \geq \lambda]$ at different levels (the connected components with measure lesser than ϵ are marked with a black cross inside) and the filtered function $SI^\epsilon u$ (note that a flat zone appears instead of the original peak).

Let $D \subseteq I\!R^N$ be a set homeomorphic to the closed unit ball of $I\!R^N$ ($N \geq 2$), $\left\{x \in I\!R^N, \|x\| \leq 1\right\}$, for instance D can be an interval in $I\!R^N$. Let $u : D \to I\!R$ be a function. Let us define two basic morphological operators, the Vincent-Serra operators, which simplify the topographic map of u by eliminating the small connected components of its upper and lower level sets. Let $\epsilon > 0$ and note by $\mathcal{CC}([u \geq \lambda], x)$ ($\mathcal{CC}([u < \lambda], x)$) the connected component of $[u \geq \lambda]$ ($[u < \lambda]$) containing x. Then, for each $x \in D$, we define

$$\mathcal{F}^\epsilon(u, x) = \{X = \mathcal{CC}([u \geq \lambda], x) : \lambda \in I\!R, |X| \geq \epsilon\},$$

$$\mathcal{F}_\epsilon(u, x) = \{X = \mathcal{CC}([u < \lambda], x) : \lambda \in I\!R, |X| > \epsilon\}.$$

Let us define the following Vincent-Serra operators

$$SI^\epsilon u(x) = \sup_{B \in \mathcal{F}^\epsilon(u,x)} \inf_{y \in B} u(y),$$

$$IS_\epsilon u(x) = \inf_{B \in \mathcal{F}_\epsilon(u,x)} \sup_{y \in B} u(y).$$

where we understand that $\sup_{B \in \mathcal{F}^\epsilon(u,x)} \inf_{y \in B} u(y) = -\infty$ if $\mathcal{F}^\epsilon(u, x) = \emptyset$ and $\inf_{B \in \mathcal{F}_\epsilon(u,x)} \sup_{y \in B} u(y) = +\infty$ if $\mathcal{F}_\epsilon(u, x) = \emptyset$. Figure 4 illustrates the filtering of a function u by the operator SI^ϵ. From left to right we have the original function u, some of the connected components of its upper level sets ($[u \geq \lambda]$) and the filtered function $SI^\epsilon u$.

Both operators can be described in terms of basis of structuring elements independent of u. Indeed, let $\mathcal{B}^\epsilon = \{B : B \text{ is connected}, 0 \in B, |B| \geq \epsilon\}$, $\mathcal{B}_\epsilon = \{B : B \text{ is connected}, 0 \in B, |B| > \epsilon\}$. Then

$$SI^\epsilon u(x) = \sup_{B \in x + \mathcal{B}^\epsilon} \inf_{y \in B} u(y), \tag{2}$$

$$IS_\epsilon u(x) = \inf_{B \in x + \mathcal{B}_\epsilon} \sup_{y \in B} u(y). \tag{3}$$

Let us denote, for the time being, the right hand side of (2) and (3) by $SI^{\epsilon,*}u(x)$, respectively, $IS_{\epsilon,*}u(x)$. Let us check that in fact $SI^{\epsilon,*}u(x) = SI^\epsilon u(x)$ and $IS_{\epsilon,*}u(x) = IS_\epsilon u(x)$. Obviously, from the definition we have that $SI^\epsilon u(x) \leq SI^{\epsilon,*}u(x)$ and $IS_\epsilon u(x) \geq IS_{\epsilon,*}u(x)$. Now, if $SI^{\epsilon,*}u(x) < \infty$, given $\delta > 0$,

let $B \in x + \mathcal{B}^\epsilon$ be such that $i_B := \inf_{y \in B} u(y) \geq SI^{\epsilon,*}u(x) - \delta$. Then $B \subseteq [u \geq i_B]$ and, therefore, $B \subseteq X := \mathcal{CC}([u \geq i_B], x)$. Hence $X \in \mathcal{F}^\epsilon(u, x)$ and

$$SI^{\epsilon,*}u(x) - \delta \leq i_B \leq \inf_{y \in X} u(y) \leq SI^\epsilon u(x).$$

In a similar way, we prove that $SI^\epsilon u(x) = \infty$ if $SI^{\epsilon,*}u(x) = \infty$. We have checked formula (2). In a similar way we prove the identity (3).

Proposition 3 *Assume that $u, v : D \to I\!R$ are measurable functions. Then*
i) $IS_\epsilon u \geq u$ and $SI^\epsilon u \leq u$.
ii) If $u \leq v$, then $IS_\epsilon u \leq IS_\epsilon v$ and $SI^\epsilon u \leq SI^\epsilon v$.
iii) $IS_\epsilon(\alpha) = SI^\epsilon(\alpha) = \alpha$ for all $\alpha \in I\!R$.
iv) $IS_\epsilon(u + \alpha) = IS_\epsilon u + \alpha$ for all $\alpha \in I\!R$. A similar statement holds for SI^ϵ.

Proof: i) Let $x \in D$. If $\mathcal{F}_\epsilon(u, x) = \emptyset$, then $IS_\epsilon u(x) = \infty$ and we are done. If $B \in \mathcal{F}_\epsilon(u, x)$, then $x \in B$, and $\sup_{y \in B} u(y) \geq u(x)$. Thus $IS_\epsilon u(x) \geq u(x)$. In the same way we prove that $SI^\epsilon u(x) \leq u(x)$.
The proof of $ii)$ follows immediately from the identities (2) and (3). The proof of assertions $iii)$ and $iv)$ is immediate and we shall omit it. □

Proposition 4 *Let $u_n, u : D \to I\!R$ be measurable functions such that $u_n \to u$ uniformly in D. Then $SI^\epsilon u_n \to SI^\epsilon u$ and $IS_\epsilon u_n \to IS_\epsilon u$ as $n \to \infty$ uniformly in D.*

Proof: Since $u_n \to u$ uniformly we have that given $\delta > 0$ there exists n_0 such that $\|u_n - u\| < \delta$ for all $n \geq n_0$, i.e. $u - \delta \leq u_n \leq u + \delta$ for all $n \geq n_0$. Using Proposition 3, (ii) and (iv), we obtain

$$SI^\epsilon u - \delta \leq SI^\epsilon u_n \leq SI^\epsilon u + \delta,$$

for all $n \geq n_0$. Hence $SI^\epsilon u_n \to SI^\epsilon u$ as $n \to \infty$ uniformly in D. Similarly, we prove that $IS_\epsilon u_n \to IS_\epsilon u$ as $n \to \infty$ uniformly in D. □

Proposition 5 *([8],[14]) If $X = \mathcal{CC}([IS_\epsilon u < \lambda], x) \neq \emptyset$, then $|X| > \epsilon$. If $X = \mathcal{CC}([SI^\epsilon u \geq \lambda], x) \neq \emptyset$, then $|X| \geq \epsilon$. If $|\mathcal{CC}([u \geq \lambda], x)| \geq \epsilon$ (resp. $|\mathcal{CC}([u < \lambda], x)| \geq \epsilon$), then $|\mathcal{CC}([IS_\epsilon u \geq \lambda], x)| \geq \epsilon$ (resp. $|\mathcal{CC}([SI^\epsilon u < \lambda], x)| \geq \epsilon$).*

Remark 2 Thus, by filtering the small connected components of the upper and lower level sets with the Vincent-Serra operators we can guarantee that the assumption of Propositions 1 and 2 is satisfied.

Remark 3 As proved in [8, 14] both operators IS_ϵ and SI^ϵ are contrast invariant operators induced by operators on sets.

The following result was also proved in [8, 14].

Proposition 6 *Assume that D is compact. Let $u : D \to I\!R$ be a continuous function. Then $IS_\epsilon u$ and $SI^\epsilon u$ are continuous. Therefore $IS_\epsilon SI^\epsilon u$ and $SI^\epsilon IS_\epsilon u$ are continuous.*

Remark 4 Motivated by the study of a family of filters by reconstruction ([31], [32], [49], [63], [62]), J. Serra and Ph. Salembier ([56], [52]) introduced the notion of connected operators. Such operators simplify the topographic map of the image. These filters have become very popular because, on an experimental basis, they have been claimed to simplify the image while preserving contours. This property has made them very attractive for a large number of applications such as noise cancellation or segmentation ([36], [64]). More recently, they have become the basis of a morphological approach to image and video compression (see [50] and references therein, and more recently [21]).

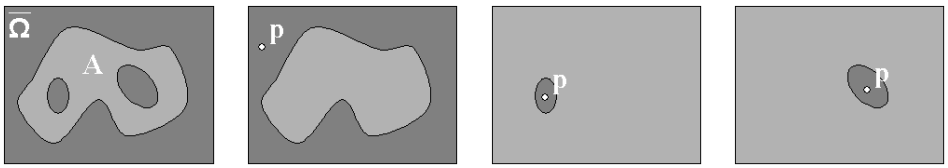

Figure 5: From left to right a set A (in light gray) and its saturations.

5 Structure of the simplified topographic map

The aim of this Section is to review the following result: Assuming that the connected components of the upper and lower level sets have minimal size $\delta > 0$, then there is only a finite number of maximal monotone sections in the topographic map of u [8, 9]. The idea being that given two of them there exists a set of area $\geq \delta$ contained between them.

Let $\overline{\Omega}$ be a set homeomorphic to the closed unit ball of $\mathbb{R}^N$ ($N \geq 2$), $\left\{x \in \mathbb{R}^N, \|x\| \leq 1\right\}$, and Ω be the interior of $\overline{\Omega}$. Note that, in particular, $\overline{\Omega}$ is compact, connected and locally connected. Moreover, $\overline{\Omega}$ is unicoherent.

Definition 2 *([29], vol. II, p. 104) A topological space Z is said to be unicoherent if it is connected and for any two closed connected sets A, B in Z such that $Z = A \cup B$ we have that $A \cap B$ is connected.*

A word of caution: when we say that, if X is a connected component of an upper or lower level set, we mean that $X = \mathcal{CC}([u \geq \lambda], p)$ or $X = \mathcal{CC}([u < \lambda], p)$ for some $\lambda \in \mathbb{R}$, $p \in \overline{\Omega}$.

5.1 Saturations

We recall the definition of saturation and prove its basic properties. The results in this subsection are taken from [8], [9], [38].

Definition 3 *Let $A \subseteq \overline{\Omega}$. We call holes of A in $\overline{\Omega}$ the components of $\overline{\Omega} \setminus A$. Let $p_\infty \in \overline{\Omega} \setminus A$ be a reference point, and let T be the hole of A in $\overline{\Omega}$ containing p_∞. We define the saturation of A with respect to p_∞ as the set $\overline{\Omega} \setminus T$ and we denote it by $sat(A, p_\infty)$. We shall refer to T as the external hole of A and to the other holes of A as its internal holes. By extension, if $p_\infty \in A$, by convention we define $sat(A, p_\infty) = \overline{\Omega}$. Note that $sat(A, p_\infty)$ is the union of A and its internal holes.*

The reference point p_∞ acts as a point at infinity. In all what follows, we assume that the point $p_\infty \in \overline{\Omega}$ on which the saturations are based is fixed, i.e., all saturations will be computed with respect to p_∞. To simplify our notation, we shall write $sat(A)$ instead of $sat(A, p_\infty)$. We shall also speak of holes of A instead of holes of A in $\overline{\Omega}$.

Lemma 1 *Saturations are always connected sets.*

Proof: Observe that by definition, since T is a connected component of the complement of A we have that $sat(A) = sat(A, T) = \overline{\Omega} \setminus T$ is also a connected set (a ([40], IV.3, Theorem 3.3). □

Figure 5 illustrates the above definition. On the left we see the original set A (light gray) which is a subset of the whole space $\overline{\Omega}$ (dark gray). Recall that the set A is also its own saturation when $p \in A$. The next three frames represent the saturations of A with respect to its three different holes.

Let us summarize the following results about saturations. They were proved in [38], [9],[8]satisusc.

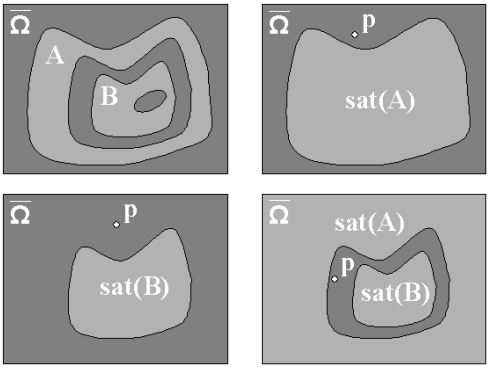

Figure 6: This figure displays the original disjoint connected sets A and B and its saturations with respect to a point p in two different situations

Lemma 2 *(i) Let $A \subseteq \overline{\Omega}$. If A is open (res. closed) in $\overline{\Omega}$, then its saturated sets are open (resp. closed) in $\overline{\Omega}$.*

(ii) The saturation is a monotonous operation, i.e., if $A \subseteq B$ and $p \in \overline{\Omega} \setminus B$, then $sat(A,p) \subseteq sat(B,p)$.

(iii) Let X be an open (closed) connected subset of $\overline{\Omega}$. Then $\partial sat(X)$ is connected.

(iv) Let $A \subseteq \overline{\Omega}$ be a connected set and T be a hole of A. If T is an internal hole, $sat(T) = T$; if T is the external hole, $sat(T) = \overline{\Omega}$.

(v) Let $A, B \subseteq \overline{\Omega}$ be connected sets such that $A \cap B = \emptyset$. Then either $sat(A) \subseteq sat(B)$, or $sat(B) \subseteq sat(A)$, or $sat(A) \cap sat(B) = \emptyset$. Moreover, if we assume that A and B are closed , then either $sat(A) \subseteq int(sat(B))$, or $sat(B) \subseteq int(sat(A))$, or $sat(A) \cap sat(B) = \emptyset$.

(vi) Let K_n be a decreasing sequence of continua, $K = \cap_n K_n$, and $p \notin K$. Then $sat(K,p) = \cap_n sat(K_n, p)$.

Part (iv) of this lemma is illustrated in Fig. 6. From left to right and top to bottom we have the original sets A and B, the saturation of A and B with respect to a point p which is external to A (observe that this case gives $sat(B) \subseteq sat(A)$) and finally the saturation of both sets when p is external to B but internal to A (which corresponds to $sat(A) \cap sat(B) = \emptyset$).

5.2 Some results on the structure of the topographic map

Lemma 3 *Let $u \in C(\overline{\Omega})$. We assume that there is some $\delta > 0$ such that, if K is a connected component of an upper or lower level set, then $|K| \geq \delta$. Then for each $\lambda \in I\!R$ there is a finite number of connected components of $[u \geq \lambda]$ and each component has a finite number of holes.*

Proof: Let $\lambda \in I\!R$. Since each connected component of $[u \geq \lambda]$ has area $\geq \delta$, there must be a finite number of them. Let Y be a component of $[u \geq \lambda]$ and let H be a hole of Y. Observe that $\partial H \subseteq \partial Y \subseteq Y$. Since $Y \cap \overline{H} \neq \emptyset$ and $Y, \overline{H}$ are connected, then $Y \cup H = Y \cup \overline{H}$ is connected. If $H \subseteq [u \geq \lambda]$, then $H \subseteq Y$, a contradiction. Hence $H \cap [u < \lambda] \neq \emptyset$. We conclude that each hole of Y contains a component of $[u < \lambda]$. Hence there may be only a finite number of them. □

The following result was proved in [8]. An analogous result for the tree of shapes of the image introduced by P. Monasse [38] was proved in [9].

Theorem 1 *Let $u : \overline{\Omega} \to I\!R$ be a continuous function. Assume that there is some $\delta > 0$ such that, if X is a connected component of an upper or lower level set, then $|X| \geq \delta$. Then*

(i) for each $\lambda, \mu \in I\!R$ with $\lambda \leq \mu$, the set $U_{\lambda,\mu}$ has a finite number of connected components, and

(ii) there is a finite number of maximal monotone sections in the topographic map of u.

According to Sect. 3 the main implication of Theorem 1, item (i), is that we may define the maximal monotone sections containing a given point. On the other hand, if u is continuous, then by the results of Sect. 4, the function $\overline{u} = IS_\delta SI^\delta u$ is also continuous and Proposition 5 holds, namely, if X is a connected component of an upper or lower level set, then $|X| \geq \delta$. One can also take $\overline{u} = SI^\delta IS_\delta u$. In any case, if a continuous function u does not satisfy the assumption of Theorem 1, then by filtering the connected components of size less than δ, these assumption are satisfied.

5.3 Some topological preliminaries

Most of the results of this Section were proved in [8]. Since in the rest of the paper we shall use some of them we include their proof. The proofs given here are simpler than the ones in [8].

Lemma 4 *Let E be a closed set with a finite number of connected components. Let $X \in \mathcal{CC}(E)$. Let L be a hole of X. Then there is some $\eta > 0$ such that $L_\eta := \{p \in L : d(p, X) < \eta\} \subseteq \overline{\Omega} \setminus E$.*

Proof: Let H be any hole of X. Since $\overline{\Omega}$ is unicoherent, $sat(X, H)$, $\overline{H}$ are closed connected sets, and $sat(X, H) \cup \overline{H} = \overline{\Omega}$, we have that $\partial H = sat(X, H) \cap \overline{H}$ is connected. We observe that $\partial H \subseteq \partial X \subseteq \partial E = \partial(\overline{\Omega} \setminus E)$. Let us prove that, for some $\eta > 0$, $\{p \in L : d(p, X) < \eta\} \subseteq \overline{\Omega} \setminus E$. Let $Y \in \mathcal{CC}(E)$, $Y \neq X$. Then either $Y \subseteq L$ or in a another hole of X. Let us consider the connected components of E which are contained in L. There are only finitely many, by our assumption on E, say $Y_1, ..., Y_k$. Since E is closed, each of Y_i is closed and $\cup_{i=1}^k Y_i$ is also closed. Since $\cup_{i=1}^k Y_i \subseteq L$ and L is open, then $d(\cup_{i=1}^k Y_i, \partial L) > 0$. Thus $d(E \cap L, \partial L) > 0$, and, therefore, there is some $\eta > 0$ such that $\{p \in L : d(p, X) < \eta\} \subseteq \overline{\Omega} \setminus E$. □

Corollary 1 *Let $u \in C(\overline{\Omega})$. Assume that there is some $\delta > 0$ such that, if K is a connected component of an upper or lower level set of u, then $|K| \geq \delta$. Let X be a connected component of $[\lambda \leq u \leq \mu]$, $\lambda \leq \mu$, and let L be a hole of X. Then there is some $\eta > 0$ such that either*
i) $sat(X, L) = sat(\mathcal{CC}([u \geq \lambda], X), L)$, and $u < \lambda$ on $L_\eta := \{p \in L : d(p, X) < \eta\}$, or
ii) $sat(X, L) = sat(\mathcal{CC}([u \leq \mu], X), L)$, and $u > \mu$ on $L_\eta := \{p \in L : d(p, X) < \eta\}$.

Proof: As in the proof of Lemma 4, we have that

$$\partial L \subseteq \partial([u < \lambda] \cup [u > \mu]) = \partial[u < \lambda] \cup \partial[u > \mu].$$

Assume that $\lambda < \mu$. Then $\partial[u < \lambda] \cap \partial[u > \mu] = \emptyset$ and, being ∂L a connected set, we have either $\partial L \subseteq \partial[u < \lambda]$ or $\partial L \subseteq \partial[u > \mu]$. Without loss of generality, we may assume that $\partial L \subseteq \partial[u < \lambda] \subseteq [u = \lambda]$. By Lemma 4 we know that there is some $\eta > 0$ such that $L_\eta \subseteq [u < \lambda] \cup [u > \mu]$. Since $u \in C(\overline{\Omega})$ and $u = \lambda$ in ∂L then, taking, η small enough we may assume that $u < \mu$ in L_η. Then we conclude that $L_\eta \subseteq [u < \lambda]$. This implies that L is a hole of $\mathcal{CC}([u \geq \lambda], X)$, and $sat(X, L) = sat(\mathcal{CC}([u \geq \lambda], X), L)$.

Let us consider the case $\lambda = \mu$. By assumption, X is a connected component of $[u = \lambda]$ and L is a hole of X. Let $y \in X$. Then $X = \cap_n X_n$ where $X_n = \mathcal{CC}([\lambda \leq u \leq \lambda + \frac{1}{n}], y)$. Let $p \in L$.

Then, by Lemma 2, vi, we know that $sat(X,p) = \cap_n sat(X_n,p)$. Without loss of generality, we may assume that $p \notin X_n$ for all $n \geq 1$. But, according to the first part of the proof, we have that either $sat(X_n,p) = sat(\mathcal{CC}([u \geq \lambda], y), p)$, or $sat(X_n,p) = sat(\mathcal{CC}([u \leq \lambda + \frac{1}{n}], y), p)$. In the first case, we conclude that $sat(X,p) = sat(\mathcal{CC}([u \geq \lambda], y), p)$. In the second case, using again Lemma 2, vi, we have that $\cap_n sat(\mathcal{CC}([u \leq \lambda + \frac{1}{n}], y), p) = sat(\mathcal{CC}([u \leq \lambda], y), p)$. Hence, $sat(X,p) = sat(\mathcal{CC}([u \leq \lambda], y), p)$.

When $sat(X,p) = sat(\mathcal{CC}([u \geq \lambda], y), p)$, L is a hole of $\mathcal{CC}([u \geq \lambda], y)$. Hence $\partial L \subseteq \partial[u < \lambda]$ and the argument above proves that there is some $\eta > 0$ such that $u < \lambda$ on $L_\eta = \{p \in L : d(p,X) < \eta\}$. When $sat(X,p) = sat(\mathcal{CC}([u \leq \lambda], y), p)$, L is a hole of $\mathcal{CC}([u \leq \lambda], y)$. Then $\partial L \subseteq \partial[u > \lambda]$ and again the previous argument proves that there is some $\eta > 0$ such that $u > \lambda$ on $L_\eta = \{p \in L : d(p,X) < \eta\}$. □

Lemma 5 *Let $u \in C(\overline{\Omega})$. Assume that there is some $\delta > 0$ such that, if K is a connected component of an upper or lower level set, then $|K| \geq \delta$. Let $\lambda \leq \mu$.*
(i) Let X be a connected component of $U_{\lambda,\mu}$, $\lambda < \mu$. Then $sat(X)$ contains either a maximum or a minimum point.
(ii) Let X, Y be two connected component of $U_{\lambda,\mu}$, $\lambda \leq \mu$, with X contained in a hole of Y. Then there is an extremum in $sat(Y) \setminus sat(X)$.

Proof: (i) If $sat(X) \cap [u > \mu] \neq \emptyset$ there is a maximum point of u in $sat(X)$. If $sat(X) \cap [u < \lambda] \neq \emptyset$ then there is a minimum point of u in $sat(X)$. Thus we may assume that $sat(X) \subseteq U_{\lambda,\mu}$. In this case, $sat(X) = X$. Observe that $\partial X \subseteq [u = \lambda] \cup [u = \mu]$. Since ∂X is connected and $[u = \lambda]$ and $[u = \mu]$ are disjoint then either $\partial X \subseteq [u = \lambda]$ or $\partial X \subseteq [u = \mu]$. If $\partial X \subseteq [u = \lambda]$, then the alternative $i)$ of Proposition 1 holds, i.e., $u < \lambda$ on $\{x \in \overline{\Omega} \setminus X : d(x,X) < \eta\}$, for some $\eta > 0$. Then X is a connected component of $[u \geq \lambda]$ and there is a maximum of u inside X. If $\partial X \subseteq [u = \mu]$, in the same way we conclude that there is a minimum of u inside X.
(ii) Let us observe that $sat(Y) \setminus sat(X)$ cannot be contained in $[\lambda \leq u \leq \mu]$. Assume on the contrary that $sat(Y) \setminus sat(X) \subseteq [\lambda \leq u \leq \mu]$. Now, since $\overline{\Omega}$ is unicoherent, $sat(Y) \setminus sat(X) = sat(Y) \cap (\overline{\Omega} \setminus sat(X))$ and both $sat(Y)$, $\overline{\Omega} \setminus sat(X)$ are connected, then $sat(Y) \setminus sat(X)$ is connected. Since $Y \cap (sat(Y) \setminus sat(X)) \neq \emptyset$ and $Y \in \mathcal{CC}([\lambda \leq u \leq \mu])$, we have that $sat(Y) \setminus sat(X) \subseteq Y$. Then $\partial sat(X) \subseteq Y$ and we conclude that $X \cap Y \neq \emptyset$. This implies that X and Y are connected inside $[\lambda \leq u \leq \mu]$, a contradiction.
We have obtained that $sat(Y) \setminus sat(X)$ must intersect either $[u < \lambda]$, in which case there is a local minimum of u inside $sat(Y) \setminus sat(X)$, or it must intersect $[u > \mu]$, in which case there is a maximum of u inside $sat(Y) \setminus sat(X)$. □

Lemma 6 *Let $u \in C(\overline{\Omega})$. Assume that there is some $\delta > 0$ such that, if K is a connected component of an upper or lower level set, then $|K| \geq \delta$. Let $\lambda \leq \mu$.*
$i)$ Let X be a connected component of $U_{\lambda,\mu}$. Then $|sat(X)| \geq \delta$.
$ii)$ Let X, Y be two connected components of $U_{\lambda,\mu}$ with X contained in a hole of Y. Suppose that both satisfy the same alternative in Corollary 1,i.e., that $u < \lambda$, or $u > \mu$, in both sets $\{p \in L_X : d(p,X) < \eta\}$ and on $\{p \in L_Y : d(p,Y) < \eta\}$, where L_X and L_Y are the external holes of X, Y, respectively. Then $|sat(Y) \setminus sat(X)| \geq \delta$.

Proof: $i)$ is a consequence of Proposition 1. To prove $ii)$, to fix ideas, let us assume that there is some $\eta > 0$ such that $u < \lambda$ on $\{p \in L_X : d(p,X) < \eta\}$ and on $\{p \in L_Y : d(p,Y) < \eta\}$, where L_X and L_Y are the external holes of X, Y, respectively. Then, there is a connected component of $[u \geq \lambda]$ contained in $sat(Y) \setminus sat(X)$, and, therefore, $|sat(Y) \setminus sat(X)| \geq \delta$. □

Definition 4 *A sequence $A_1, \ldots, A_p$ of subsets of $\overline{\Omega}$ is called a chain if each A_i is contained in an internal hole of A_{i-1}, $i = 2, \ldots, p$.*

Lemma 7 *Let $u \in C(\overline{\Omega})$. Assume that there is some $\delta > 0$ such that if X is a component of an upper or lower level set, then $|X| \geq \delta$. Let $J \subseteq I\!N$. Let K_j, $j \in J$, be a connected component of U_{α_j,β_j}, $\alpha_j \leq \beta_j$, such that $K_i \cap K_j = \emptyset$ for all $i \neq j$, $i, j \in J$.*
i) For each $j \in J$ let T_i^j, $i = 1, \ldots, h_j$, be the holes K_j containing some K_i, $i \in J$. Then

$$|\cup_{i=1}^{h_j} T_i^j| \geq h_j \delta.$$

In particular

$$\sup_j h_j \leq \frac{|\Omega|}{\delta}.$$

ii) Suppose that J is countable. Then (we may fix the point of infinity so that) there is an infinite chain formed by sets of the family K_j.

Proof: i) Suppose that T_i^j contains $K_{n_i^j}$. Then, it contains also a saturation of $K_{n_i^j}$. Thus, by Lemma 6, $|sat(K_{n_i^j})| \geq \delta$. This implies the statement of the present Lemma.
ii) Let $j \in J$. Observe that the number of K_i in the holes (i.e., the components of its complement) of K_j is infinite. By i), there is a hole of K_j which contains an infinite number of K_i. Let T^1 be this hole. Fix as a point of infinity a point $p \notin T_1$ and we take saturations with respect to p. Suppose that there is an infinity of K_i, K_{i_r}, in T^1 such that $sat(K_{i_r})$ are two by two disjoint. Using Lemma 6, i), we obtain that

$$|T^1| \geq k\delta$$

for all $k \geq 1$, a contradiction. Thus there is only a finite system of components K_i such that $sat(K_i)$ are two by two disjoint. Then one of them, say K_{i_1}, contains an infinity of $K_i's$ in his system of internal holes. Again, by the previous argument, there is an internal hole of K_{i_1}, say T^2, containing an infinite number of K_i. Repeating the same argument we find a subsequence K_{i_n}, $n = 1, 2, \ldots$, such that $K_{i_{n+1}}$ is contained in an internal hole of K_{i_n}. □

6 Critical and singular values

This section is devoted to the definition of critical and singular values. Critical values are defined as the levels where a monotone section begins or ends. This definition is adapted to the algorithm that we have developed to compute the maximal monotone sections (see Section 6.1). In addition, we will prove that the critical and singular values are equivalent.

Throughout this section we shall assume that $u \in C(\overline{\Omega})$ and there is some $\delta > 0$ such that, if K is a connected component of an upper or lower level set, then $|K| \geq \delta$. We recall that, by Lemma 3, each level set has a finite number of connected components and a finite number of holes.

Definition 5 *Let $\lambda \in I\!R$. The signature of the level set $[u \geq \lambda]$ (resp. $[u < \lambda]$) consists of a finite family of points $\{p_i : i = 1, ..., r\}$ (resp. $\{q_j : j = 1, ..., s\}$) such that each p_i (resp. q_j) is a point in a different connected component $X^{\lambda,i}$ (resp. $X_{\lambda,j}$) of $[u \geq \lambda]$ (resp. $[u < \lambda]$). The points p_i, q_j are selected so that*

$$u(p_i) = \sup_{x \in X^{\lambda,i}} u(x), \text{ and } \quad u(q_j) = \inf_{x \in X_{\lambda,j}} u(x).$$

We shall denote the signature of $[u \geq \lambda]$ by $sig([u \geq \lambda])$, the signature of $[u < \lambda]$ by $sig([u < \lambda])$. We define $sig([u \geq \lambda], [u < \lambda]) = sig([u \geq \lambda]) \cup sig([u < \lambda])$.

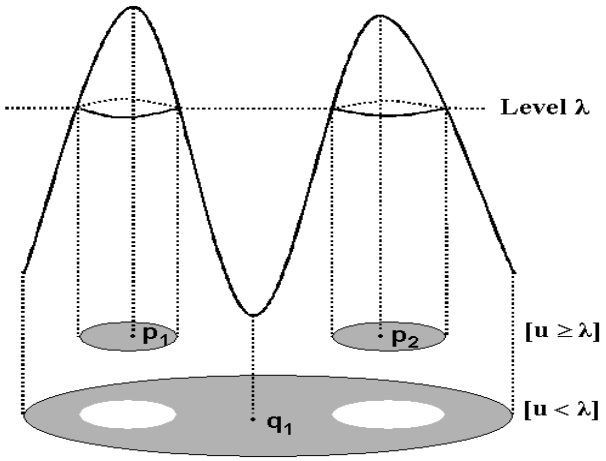

Figure 7: A function u and its upper and lower level sets at level λ with its assigned signature.

Figure 7 illustrates the above definition. Note that in the case presented in this figure, $sig([u \geq \lambda]) = \{p_1, p_2\}$, $sig([u < \lambda] =)\{q_1\}$ and $sig([u \geq \lambda], [u < \lambda]) = \{p_1, p_2, q_1\}$.

Let $\lambda < \mu$. If $sig([u \geq \lambda], [u < \lambda]) \neq sig([u \geq \mu], [u < \mu])$, then either (a) $sig([u \geq \lambda]) \neq sig([u \geq \mu])$ or (b) $sig([u < \lambda]) \neq sig([u < \mu])$. Suppose that (a) holds. Since $[u \geq \mu] \subseteq [u \geq \lambda]$ each connected component of $[u \geq \mu]$ is contained in a component of $[u \geq \lambda]$. Two critical phenomena may happen: (a_1) there are two different components of $[u \geq \mu]$ which are contained in the same component of $[u \geq \lambda]$, i.e., two connected components of $[u \geq \mu]$ merged at level λ, or (a_2) there is a component of $[u \geq \lambda]$ with no component of $[u \geq \mu]$ contained in it, i.e., a new connected component of the upper level sets appeared at level $[u \geq \lambda]$. Suppose that (b) holds. Since $[u < \lambda] \subseteq [u < \mu]$, each component of $[u < \lambda]$ is contained in a component of $[u < \mu]$. Again, the same two critical phenomena may happen: (b_1) there are two different connected components of $[u < \lambda]$ which are contained in the same component of $[u < \mu]$, i.e., a connected component of $[u < \mu]$ has splitted at level λ, (b_2) there is a component of $[u < \mu]$ with no component of $[u < \lambda]$ contained in it, i.e., a connected component of the lower level sets is present at level μ while it was absent at level λ.

Lemma 8 *Let $\lambda \in I\!R$. There is $\epsilon > 0$ such that $sig([u \geq \mu], [u < \mu])$ is constant for all $\mu \in (\lambda - \epsilon, \lambda]$.*

Proof: Let $X^{\lambda,i}$, $X_{\lambda,j}$, $i = 1, ..., r$, $j = 1, ..., s$, be the the family of connected components of $[u \geq \lambda]$, resp. $[u < \lambda]$ with the markers p_i, q_j defined above. Let $i \in \{1, ..., r\}$. For each $\mu < \lambda$, let $X^{\mu,i}$ be the connected component of $[u \geq \mu]$ containing $X^{\lambda,i}$. Then, obviously, we have

$$X^{\lambda,i} \subseteq \cap_{\mu<\lambda} X^{\mu,i}.$$

Now, since $X^{\mu,i}$ is a decreasing sequence of continua their intersection is also a continuum. Moreover, it is contained in $[u \geq \lambda]$. Therefore,

$$\cap_{\mu<\lambda} X^{\mu,i} \subseteq \mathcal{CC}([u \geq \lambda], p_i) = X^{\lambda,i},$$

and we have the equality of both sets. As a consequence, there is an $\epsilon > 0$ such that for each $\mu \in (\lambda - \epsilon, \lambda]$, the sets $X^{\lambda,i}$, $i = 1, ..., r$, are contained in different connected components of $[u \geq \mu]$. Moreover, it cannot exist a sequence of values $\mu_n \uparrow \lambda$ such that $[u \geq \mu_n]$ has a connected component Q_n disjoint to $[u \geq \lambda]$. In that case $[u \geq \mu_n] \supseteq [u \geq \lambda] \cup Q_n$, and, thus

$$|[u \geq \mu_n]| \geq |[u \geq \lambda]| + \delta.$$

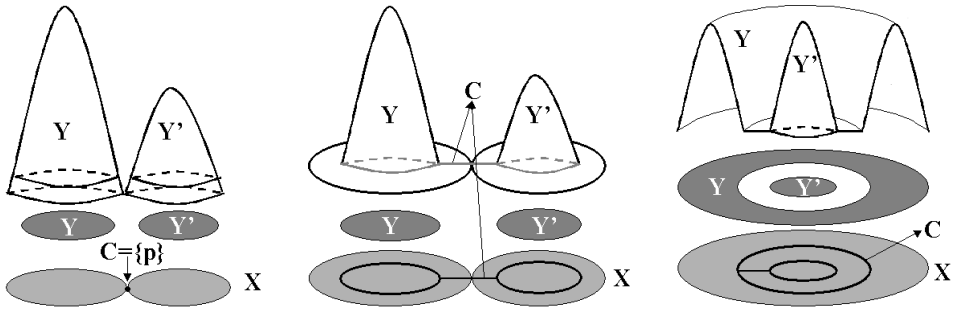

Figure 8: From left to right we present three different cases that may happen when considering the hypothesis of Lemmas 9 and 10.

Since $[u \geq \mu_n] \downarrow [u \geq \lambda]$, also $|[u \geq \mu_n]| \downarrow |[u \geq \lambda]|$. This contradiction proves that there is an $\epsilon > 0$ such that for each $\mu \in (\lambda - \epsilon, \lambda]$ the set $[u \geq \mu]$ consists of r connected components, each one of them containing a different component of $[u \geq \lambda]$.

Let $\mu_n \uparrow \lambda$. Again, using that $\cup_n [u < \mu_n] = [u < \lambda]$, for n large enough, we have that $[u < \mu_n] \cap X_{\lambda,j}$, $j = 1, ..., s$, are the connected components of $[u < \mu_n]$. We conclude that there is an $\epsilon > 0$ such that $sig([u \geq \mu], [u < \mu])$ is constant for each $\mu \in (\lambda - \epsilon, \lambda]$. □

Definition 6 *We say that $\lambda \in \mathbb{R}$ is a critical value for u if there is a sequence $\mu_n \downarrow \lambda$ such that $sig([u \geq \mu_n], [u < \mu_n]) \neq sig([u \geq \lambda], [u < \lambda])$ for each $n = 1, 2, ...$*

Definition 7 *Let $M \subseteq \overline{\Omega}$. We say that M is a zonal maximum (resp., minimum) of u at height λ if M is a connected component of $[u = \lambda]$ and, for all $\epsilon > 0$, the set $[\lambda - \epsilon < u \leq \lambda]$ (resp., $[\lambda \leq u < \lambda + \epsilon]$) is a neighborhood of M.*

Definition 8 *We say that $\lambda \in \mathbb{R}$ is a singular value if it corresponds to a zonal maximum, minimum, or it corresponds to a level where it begins or ends a maximal monotone section, i.e., there is a point $x \in \overline{\Omega}$ such that $\eta_+(x, \lambda) = \lambda$ or $\eta_-(x, \lambda) = \lambda$.*

Remark 5 Observe that the definition of singular value is self-dual, in the sense that, λ is a singular value of u if and only if $-\lambda$ is a singular value of $-u$.

Proposition 7 *If $\lambda \in \mathbb{R}$ is a critical value, then λ is also a singular value.*

We shall need the following two Lemmas. Similar results, though in a different context, were proved in [8].

Let A, B be two closed connected sets such that $A \cap B = \emptyset$. If $sat(A) \cap sat(B) = \emptyset$, then we define $Q(A) = \partial sat(A)$, $Q(B) = \partial sat(B)$. If $sat(A) \subseteq sat(B)$, then $sat(A)$ is contained in a hole H of B. Take a point $p \in H \setminus sat(A)$. Then $sat(A, p) \cap sat(B, p) = \emptyset$ and we define $Q(A) = \partial sat(A, p)$, $Q(B) = \partial sat(B, p)$. In a similar way, we define $Q(A)$ and $Q(B)$ when $sat(B) \subseteq sat(A)$.

Figure 8 illustrates Lemmas 9 and 10 by presenting three different cases where the hypothesis of these lemmas hold. At the top of the figure we can see the considered cases (different functions u), in the middle the associated sets Y and Y' and finally the set X containing the continuum C for each case.

Lemma 9 *Let $u \in C(\overline{\Omega})$. Let $\lambda \in \mathbb{R}$. Suppose that X is a connected component of $[u \geq \lambda]$ such that $[u > \lambda] \cap X$ is not connected. Then there exist $Y, Y' \in \mathcal{CC}([u > \lambda] \cap X)$, $Y \neq Y'$, such that $\overline{Y}, \overline{Y'}$ are classically connected inside X by a continuum $C \subseteq [u = \lambda]$. If $\overline{Y} \cap \overline{Y'} = \emptyset$, then we may assume that $C \supseteq Q(\overline{Y}) \cup Q(\overline{Y'})$.*

Proof 1: If A, B are two connected components of $[u > \lambda] \cap X$ such that $\overline{A} \cap \overline{B} \neq \emptyset$, then we may take $C = \{p\}$ for some point $p \in \overline{A} \cap \overline{B}$. Thus, we may assume that $\overline{A} \cap \overline{B} = \emptyset$, for any two connected components A, B of $[u > \lambda] \cap X$.

Let us denote by $Y_1, ..., Y_n$ the connected components of $[u > \lambda] \cap X$. By the results above we know that there is only a finite number of connected components of $[u = \lambda] \cap X$, let them be $\Lambda_1, ..., \Lambda_m$. By last paragraph, we may assume that $\overline{Y}_1, ..., \overline{Y}_n$ are two by two disjoint. Obviously $X = \cup_{i=1}^n \overline{Y}_i \cup \cup_{j=1}^m \Lambda_j$. Suppose that each Λ_i intersects at most one of the $\overline{Y}_i$, $i = 1, ..., n$. Since $\partial Y_i \subseteq [u = \lambda]$, given $\overline{Y}_i$, $i = 1, ..., n$, there is some Λ_{k_i}, $k_i \in \{1, .., m\}$, such that $\overline{Y}_i \cap \Lambda_{k_i} \neq \emptyset$. Suppose that there is some $k \in \{1, ..., m\} \setminus \{k_1, .., k_n\}$. Since Λ_k are closed sets and X is connected, it cannot happen that Λ_k does not intersect $\cup_{i=1}^n \overline{Y}_i \cup \Lambda_{k_i}$. On the other hand, Λ_k does not intersect $\cup_{i=1}^n \overline{Y}_i \cup \Lambda_{k_i}$. We conclude that $m = n$ and $\{k_1, ..., k_n\} = \{1, ..., n\}$. Since the sets $\overline{Y}_i \cup \Lambda_{k_i}$ are closed, two by two disjoint and $X = \cup_{i=1}^n \overline{Y}_i \cup \Lambda_{k_i}$, we have a contradiction. Thus, we may assume that some Λ_k intersects at least two sets $\overline{Y}_j$ and $\overline{Y}_r$. Since Λ_k is a continuum and $\overline{Y}_j$ and $\overline{Y}_r$ do not intersect, there is a point $p \in \Lambda_k \setminus (\overline{Y}_j \cup \overline{Y}_r)$. We claim that

$$\partial sat(\overline{Y_j}, p) \cap \Lambda_k \neq \emptyset, \ \partial sat(\overline{Y_r}, p) \cap \Lambda_k \neq \emptyset. \tag{4}$$

Assume, by contradiction, that $\partial sat(\overline{Y_j}, p) \cap \Lambda_k = \emptyset$. Since $\overline{Y_j} \cap \Lambda_k \neq \emptyset$, we have that $sat(\overline{Y_j}, p) \cap \Lambda_k \neq \emptyset$. Since Λ_k is a continuum, this implies that $\Lambda_k \subseteq int(sat(\overline{Y_j}, p))$. Since $p \in \Lambda_k$, we have that $p \in sat(\overline{Y_j}, p)$, a contradiction. This implies that $\partial sat(\overline{Y_j}, p) \cap \Lambda_k \neq \emptyset$. Similarly we prove the other assertion of (4). Since $\partial sat(\overline{Y_j}, p)$,and $\partial sat(\overline{Y_r}, p)$ are continuum contained in $[u = \lambda]$, we conclude that both sets are contained in Λ_k. This proves the Lemma. □

Lemma 10 *Let $u \in C(\overline{\Omega})$. Let $\lambda \in I\!R$. Suppose that X is a connected component of $[u \geq \lambda]$ such that $[u > \lambda] \cap X$ is not connected. Let $Y, Y' \in \mathcal{CC}([u > \lambda] \cap X)$, $Y \neq Y'$, be such that $\overline{Y}, \overline{Y'}$ are classically connected inside X by a continuum $C \subseteq [u = \lambda]$. If $\overline{Y} \cap \overline{Y'} \neq \emptyset$, let $C = \{x'\}$ where $x' \in \overline{Y} \cap \overline{Y'}$. If $\overline{Y} \cap \overline{Y'} = \emptyset$ we assume that $C \supseteq Q(\overline{Y}) \cup Q(\overline{Y'})$. Let $x \in C$. Then $\eta_+(u, x, \lambda) = \lambda$.*

Proof: Let $\alpha > \lambda$. Let Y_α, Y'_α be connected components of $\overline{Y} \cap [u \geq \alpha], \overline{Y'} \cap [u \geq \alpha]$. Note that $Y_\alpha \subseteq \overline{Y}$, $Y'_\alpha \subseteq \overline{Y'}$, and $Y_\alpha = \mathcal{CC}([u \geq \alpha], Y_\alpha)$, $Y'_\alpha = \mathcal{CC}([u \geq \alpha], Y'_\alpha)$. Let $\lambda < \mu \leq \alpha$. Let $Y_\mu = \mathcal{CC}([u \geq \mu], Y_\alpha)$, $Y'_\mu = \mathcal{CC}([u \geq \mu], Y'_\alpha)$. Observe that $Y_\mu \subseteq Y$, $Y'_\mu \subseteq Y'$.

In case $x' \in \overline{Y} \cap \overline{Y'}$ and $C = \{x'\}$ observe that $x' \in \partial\overline{Y} \cap \partial\overline{Y'}$. In any case, let $x \in C$. Suppose that $\eta_+(u, x, \lambda) > \lambda$ where $\eta_+(u, ., .)$ denotes the η_+, defined in Sect. 3, corresponding to u. Let $\lambda < \mu < \hat{\mu} < \eta < \eta_+(u, x, \lambda)$. Let $X_{\lambda,x} = \mathcal{CC}(\{z \in \overline{\Omega} : u(z) \in [\lambda, \eta_+(u, x, \lambda)]*\}, x)$. Let $X_{\lambda,\eta} = \{z \in X_{\lambda,x} : \lambda \leq u(z) \leq \eta\}$ (a connected set). Note that $\{z \in X_{\lambda,x} : \mu \leq u(z) \leq \hat{\mu}\}$ is a nonempty set.

Let $p_0 \in \partial\overline{Y}$, with $p_0 = x'$ in case $\overline{Y} \cap \overline{Y'} \neq \emptyset$ and $p_0 \in Q(\overline{Y})$ in case $\overline{Y} \cap \overline{Y'} = \emptyset$. Observe that $p_0 \in C \subseteq X_{\lambda,\eta}$. Let $p_1 \in Y_\mu$, and let K be a continuum contained in $\overline{Y}$ joining p_0 and p_1.

Now, we claim that there is a point $p \in \overline{Y} \cap X_{\lambda,\eta}$ such that $\mu \leq u(p) \leq \hat{\mu}$. Let $L_0 = \{y \in K : u(y) < \mu\}$, $L_1 = \{y \in K : u(y) > \hat{\mu}\}$. Observe that both are open sets in K and $L_0 \subseteq \overline{Y}$. Since $u(p_0) = \lambda < \mu$, and $u(p_1) \geq \mu$, then $p_0 \in L_0$, $p_1 \notin L_0$. Then L_0 is a neighborhood of p_0 in K. We observe that $L_0 \subseteq [\lambda \leq u \leq \eta]$. Indeed, since $L_0 \subseteq K \subseteq \overline{Y}$, then $u(y) \geq \lambda$ for all $y \in L_0$, and, on the other hand, $u(y) < \mu < \eta$, for all $y \in L_0$. Given $k \geq 1$, there is a finite sequence of points $p_0^k, p_1^k, ..., p_{N_k}^k$ in K with $p_0^k = p_0$, $p_{N_k}^k = p_1$, and $d(p_i^k, p_{i+1}^k) < \frac{1}{k}$. Let j_k be the first index i such that $p_i^k \in L_0$ and $p_{i+1}^k \notin L_0$. Observe that $j_k \leq N_k - 1$. Since K is a compact set, we may assume that $p_{j_k}^k \to p$ as $k \to \infty$. Then, also $p_{j_k+1}^k \to p$. Since $u(p_{j_k}^k) < \mu$ and $u(p_{j_k+1}^k) \geq \mu$, we have that $u(p) = \mu$. On the other hand, $p \in \overline{L_0} \subseteq [\lambda \leq u \leq \eta]$, and, being limit of points not in L_0, then $p \neq p_0$. Let $m \geq 1$, and let $k_0 \geq m$ be such that $|p_{j_k}^k - p| < \frac{1}{m}$ for all $k \geq k_0$. Recall that $p_i^k \in L_0$ for all $i \leq j_k$ and $d(p_i^k, p_{i+1}^k) \leq \frac{1}{k} \leq \frac{1}{m}$ for all i. Let γ_k be the polygonal joining p_i^k to p_{i+1}^k for all $0 \leq i \leq j_k$. Then $\sup_{p' \in \gamma_k} d(p', \overline{L_0}) \leq \frac{1}{m}$. Since

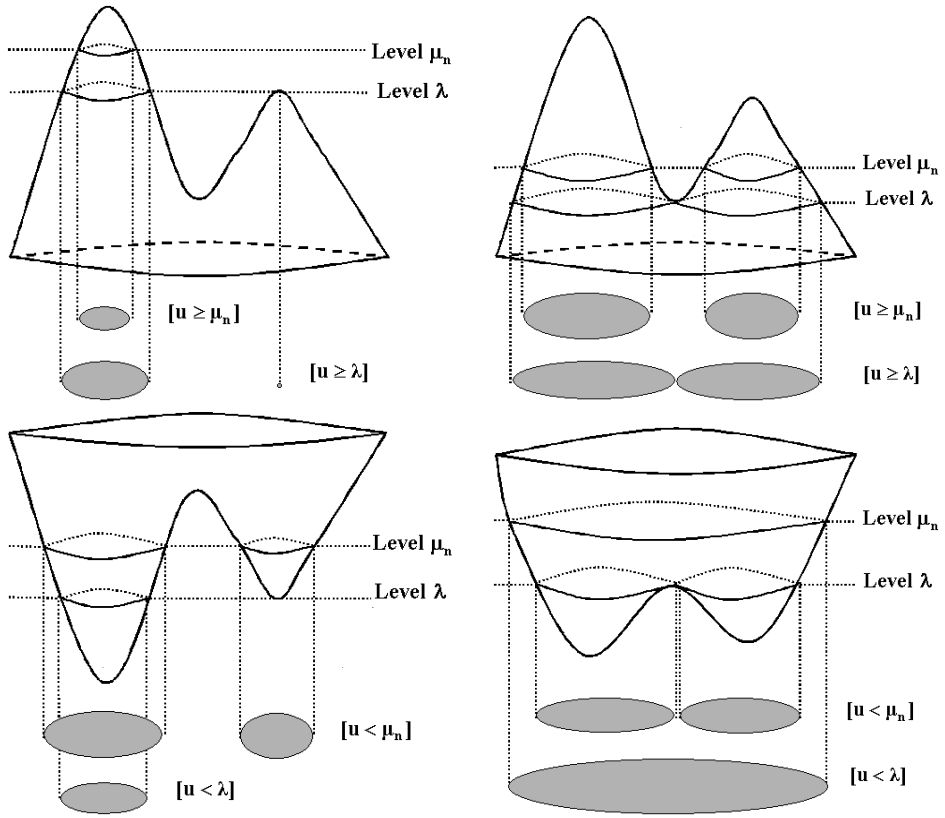

Figure 9: From left to right and top to bottom, the four cases (i) to (iv) considered in the proof of Proposition 7.

$p_0 \in \gamma_k$ for all k, $p_0 \in \liminf_k \gamma_k$. Then $\limsup \gamma_k$ is a continuum ([29], vol. II, p. 111) joining p_0 to p such that $\limsup_k \gamma_k \subseteq \overline{L_0} \subseteq \overline{Y} \cap [\lambda \leq u \leq \eta]$. Since $p_0 \in X_{\lambda,\eta}$ we conclude that $p \in \overline{Y} \cap X_{\lambda,\eta}$. In a similar way we prove that there is some $q \in \overline{Y'} \cap X_{\lambda,\eta}$ such that $\mu \leq u(q) \leq \hat{\mu}$.

Summarizing, we have shown that the sets $Y_{\mu,\hat{\mu}} := \{z \in \overline{Y} \cap X_{\lambda,\eta} : \mu \leq u(z) \leq \hat{\mu}\}$, $Y'_{\mu,\hat{\mu}} := \{z \in \overline{Y'} \cap X_{\lambda,\eta} : \mu \leq u(z) \leq \hat{\mu}\}$ are non empty. Since $X_{\lambda,x}$ is a monotone section, we have that the set $X_{\lambda,x} \cap [\mu \leq u \leq \hat{\mu}]$ is connected, and it contains $Y_{\mu,\hat{\mu}}$ and $Y'_{\mu,\hat{\mu}}$. Thus, let Q be a continuum connecting $Y_{\mu,\hat{\mu}}$ to $Y'_{\mu,\hat{\mu}}$ and contained in $X_{\lambda,x} \cap [\mu \leq u \leq \hat{\mu}]$. Observe that $u \geq \mu$ on Q. Thus $Q \subseteq \{p \in \overline{\Omega} : u > \lambda\}$ which is an open set in $\overline{\Omega}$. Thus, Y would be connected to Y' inside $[u > \lambda]$ by an open set. This contradicts the fact that Y, Y' are two different connected components of $[u > \lambda] \cap X$. This contradiction proves that $\eta_+(u, x, \lambda) = \lambda$. □

Proof of Proposition 7: Let $\mu_n > \lambda$ be such that $\mu_n \downarrow \lambda$ and $sig([u \geq \mu_n], [u < \mu_n]) \neq sig([u \geq \lambda], [u < \lambda])$ for all n. By taking a subsequence, if necessary, we may assume that either $sig([u \geq \mu_n]) \neq sig([u \geq \lambda])$ for all n, or $sig([u < \mu_n]) \neq sig([u < \lambda])$ for all n. As described after Definition 5, again, modulo a subsequence, we may assume that one of the following situations happens (see Fig. 9):

(i) for each μ_n, there is a connected component of $[u \geq \lambda]$ which does not contain a connected component of $[u \geq \mu_n]$

(ii) for each μ_n there are two connected components of $[u \geq \mu_n]$ contained in the same connected component of $[u \geq \lambda]$

(iii) for each μ_n, there is a connected component of $[u < \mu_n]$ which contains no connected component of $[u < \lambda]$

(iv) for each μ_n there are two connected components of $[u < \lambda]$ which are connected in $[u < \mu_n]$.

Assume that we are in case (i). For each μ_n there is $X_n \in \mathcal{CC}([u \geq \lambda])$ such that X_n does not contain a connected component of $[u \geq \mu_n]$. Since the number of connected components of $[u \geq \lambda]$ is finite, by taking a subsequence, if necessary, we may assume that $X_n = X \in \mathcal{CC}[u \geq \lambda])$ is independent of n. It follows that the level λ contains a zonal maximum of u, thus, it is a singular value of u. Assume that we are in case (iii). For each μ_n there is $X_n \in \mathcal{CC}([u < \mu_n])$ such that X_n contains no connected component of $[u < \lambda]$. Since for each n we have $\mu_{n+1} < \mu_n$ then $[u < \mu_{n+1}] \subseteq [u < \mu_n]$. Assume that for each $n \in I\!N$, there is an $m \geq n$ such that $X_n \cap [u < \mu_m] = \emptyset$. Then we find a sequence m_i such that $m_{i+1} < m_i$ for all i and X_{m_i} are two by two disjoint. Since each X_{m_i} has measure $\geq \delta$ this would imply an infinite measure for $\overline{\Omega}$. Hence we may assume that there is an $n_0 \in I\!N$ such that for each $n \geq n_0$ we have that $X_{n_0} \cap [u < \mu_n] \neq \emptyset$. Repeating the above argument inside X_{n_0} we find $n_1 > n_0$ and $X_{n_1} \in \mathcal{CC}([u < \mu_{n_1}])$ with $X_{n_1} \subseteq X_{n_0}$ such that for all $n \geq n_1$ we have that $X_{n_1} \cap [u < \mu_n] \neq \emptyset$. In this way we construct a sequence X_{n_i} such that $X_{n_{i+1}} \subseteq X_{n_i}$ and each X_{n_i} does not contain a connected component of $[u < \lambda]$. This implies that there is a zonal (local) minimum at level λ contained in all X_{n_i}. We deduce that λ is a singular value of u.
Suppose that we are in case (ii), i.e., for each μ_n the set $[u \geq \mu_n] \cap X$ contains two different connected components, which are components of $[u \geq \mu_n]$. Let us inductively choose these connected components. Let Y_1, Y_1' be two different connected components of $[u \geq \mu_1]$. Suppose that we have already chosen Y_i, Y_i' for all $i \leq n$. Since $[u \geq \mu_n] \subseteq [u \geq \mu_{n+1}]$, if $\mathcal{CC}([u \geq \mu_{n+1}], Y_n) \cap \mathcal{CC}([u \geq \mu_{n+1}], Y_n') = \emptyset$, we take $Y_{n+1} = \mathcal{CC}([u \geq \mu_{n+1}], Y_n)$, $Y_{n+1}' = \mathcal{CC}([u \geq \mu_{n+1}], Y_n')$. If $\mathcal{CC}([u \geq \mu_{n+1}], Y_n) = \mathcal{CC}([u \geq \mu_{n+1}], Y_n')$ then we take $Y_{n+1} = \mathcal{CC}([u \geq \mu_{n+1}], Y_n)$ and Y_{n+1}' a different connected component of $[u \geq \mu_{n+1}]$. Call this a bifurcation. We note that this bifurcation cannot happen an infinite number of times since this would amount to an infinite area contained in $[u \geq \lambda]$ because this set would contain an infinite number of connected components, two by two disjoint, of the sets $[u \geq \mu_n]$. Thus, we may assume that the families of sets Y_n and Y_n' are increasing. Let

$$Y = \cup_n Y_n \quad Y' = \cup_n Y_n'.$$

Then Y and Y' are different connected components of $[u > \lambda] \cap X$. Indeed, if p_1, p_2 are such that $u(p_1) = \max_Y u$, $u(p_2) = \max_{Y'} u$, then

$$Y = \mathcal{CC}([u > \lambda], p_1), \quad Y' = \mathcal{CC}([u > \lambda], p_2).$$

Thus, the set $[u > \lambda] \cap X$ is not connected. By Lemma 9, there exist two connected components Z, Z' of $[u > \lambda] \cap X$ satisfying the properties stated in that Lemma. Now, by Lemma 10, there is a point $x \in X$ such that $\eta_+(u, x, \lambda) = \lambda$, i.e., λ is a singular value of u.

Finally, assume that we are in case (iv). Let X_n be the connected component of $[u < \mu_n]$ which contains two different connected components A_n, B_n of $[u < \lambda]$. Since the number of connected components of $[u < \lambda]$ is finite, also is finite the number of pairs of them. Thus, by extracting a subsequence, if necessary, we may assume that X_n contains two different connected components A, B of $[u < \lambda]$ which do not depend on n. Since $\mu_{n+1} < \mu_n$ we have that $X_{n+1} \subseteq X_n$. Let $\mu_{n+1} < \mu_n' < \mu_n$. Then, if $X_n' = \mathcal{CC}([u \leq \mu_n'], A)$, then $X_{n+1} \subseteq X_n' \subseteq X_n$, and therefore $X_n' = \mathcal{CC}([u \leq \mu_n'], A \cup B)$ and

$$\cap_n X_n = \cap_n X_n'.$$

Since X_n' are compact and connected, also $\cap_n X_n'$ is, and we have that

$$\cap_n X_n' = \mathcal{CC}([u \leq \lambda], A \cup B) =: X.$$

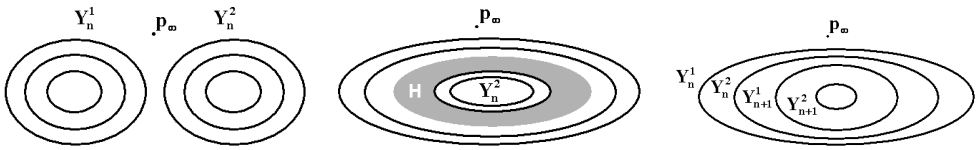

Figure 10: From left to right the three cases (i) to (iii) considered in the proof of Proposition 8.

Now we observe that $[u < \lambda]$ has two components in X. By defining $v = -u$, and applying Lemmas 9 and 10, we obtain a point $x \in X$ such that $\eta_-(u, x, \lambda) = \lambda$. We conclude that λ is a singular value of u. □

One of the consequences of Proposition 7 is that the number of critical values of u is finite. Thus the signature of $[u \geq \lambda]$ is locally constant at each side of a critical value, i.e., if λ is a critical value, then there is $\epsilon > 0$ such that

$$sig([u \geq \mu]) = sig([u \geq \lambda]) \neq sig([u \geq \mu']) \quad \text{and } sig([u \geq \mu']) \text{ is constant}$$

for each $\mu < \lambda < \mu'$, $\mu \in (\lambda - \epsilon, \lambda)$, $\mu' \in (\lambda, \lambda + \epsilon)$.

Proposition 8 *Let $\lambda \in I\!R$. If λ is a singular value of u, then λ is a critical value of u.*

Proof: Suppose that λ is a singular value which corresponds to a maximum value. Then there is a connected component X of $[u \geq \lambda]$ which does not intersect any connected component of $[u \geq \mu]$ for all $\mu > \lambda$. Let $p \in X$ be its marker. Then $p \in sig([u \geq \lambda])$ and $p \notin sig([u \geq \mu])$ for any $\mu > \lambda$. Thus λ is a critical value of u.

If λ is a minimum value, there is $q \in [u = \lambda]$ such that, if $\mu > \lambda$, then $\mathcal{CC}([u < \mu], q) \neq \emptyset$ and $\mathcal{CC}([u < \lambda], q) = \emptyset$. Then $q \in sig([u < \mu])$, $q \notin sig([u < \lambda])$. Thus λ is a critical value of u.

Now, suppose that $\eta_+(x, \lambda) = \lambda$. Then there is $X \in \mathcal{CC}([u = \lambda])$ such that $X^\epsilon := \mathcal{CC}([\lambda \leq u \leq \lambda + \epsilon], X)$ is not a monotone section for any $\epsilon > 0$. Since $\cap_{\epsilon > 0} X^\epsilon = X$, for $\epsilon > 0$ small enough we have that the only connected component of $[u = \lambda]$ contained in X^ϵ is X. Take such an ϵ. By Proposition 1 we find a sequence $\mu_n \downarrow \lambda$ such that $X^\epsilon \cap [u = \mu_n]$ are not connected. Let Y_n^1, Y_n^2 be two connected components of $X^\epsilon \cap [u = \mu_n]$. Let $Z = \mathcal{CC}([u \geq \lambda], X)$, $Z_n^1 = \mathcal{CC}([u \geq \mu_n], Y_n^1)$, $Z_n^2 = \mathcal{CC}([u \geq \mu_n], Y_n^2)$. Observe that, since $Y_n^1, Y_n^2 \subseteq X^\epsilon \subseteq Z$, we have $Z_n^1, Z_n^2 \subseteq Z$. If we prove that $Z_n^1 \neq Z_n^2$ for n large enough, we conclude that $sig([u \geq \lambda]) \neq sig([u \geq \mu_n])$, and, therefore, λ is a critical value of u. By Lemma 7 we may assume that there is a chain formed by the sets Y_n^1 and a chain formed by the sets Y_n^2 (first, take a subsequence of Y_n^1 with indexes n_i such that $Y_{n_i}^1$ is a chain, then take a subsequence n_{i_j} of n_i such that $Y_{n_{i_j}}^2$ is a chain). By extracting a subsequence we may assume that $\liminf Y_n^i \neq \emptyset$. Then $Y^i := \limsup Y_n^i$ is a continuum ([29], vol. II, p. 111). Observe that $Y^i \subseteq X_\epsilon \cap [u = \lambda] \subseteq X$, $i = 1, 2$. Let us also observe that if Y_n^1 is contained in a hole of Y_n^2 then, by Lemma 6, there is a connected component of $[u < \mu_n]$, or a connected component of $[u > \mu_n]$, in between both sets, thus, the set in between has area $\geq \delta$. By extracting subsequences, if necessary, we may assume that one of the following cases happens (see Fig. 10):

(i) the two chains have disjoint saturations

(ii) there is a hole in all sets of the first chain and containing the second chain

(iii) the two chains are intertwined, i.e., all sets Y_n^1, Y_n^2 form part of the same chain and no subsequence satisfies (ii).

Assume first that one of the chains, say Y_n^1 is increasing while the other, say Y_n^2 is decreasing. We know that, by extracting a subsequence, if necessary, we have either (a) $sat(Y_n^1) \subseteq sat(Y_n^2)$ for all n, or (b) $sat(Y_n^2) \subseteq sat(Y_n^1)$ for all n, or (c) $sat(Y_n^1) \cap sat(Y_n^2) = \emptyset$ for all n. If (a) or (b) hold, we are in case (ii). If (c) holds, we are in case (i).

Let us prove that one of the alternatives $(i) - (ii) - (iii)$ hold in case that both chains Y_n^1 and Y_n^2 are decreasing. If, for some n the saturations of Y_n^1 and Y_n^2 are disjoint, then we are in case (i). Thus we may assume that for each n, the saturations of Y_n^1 and Y_n^2 are not disjoint. Then either Y_n^1 is contained in a hole of Y_n^2, or Y_n^2 is contained in a hole of Y_n^1. By extracting a subsequence, if necessary, we may assume that Y_n^1 is contained in a hole of Y_n^2 for all n, or Y_n^2 is contained in a hole of Y_n^1 for all n. To fix ideas, let us assume that Y_n^2 is in a hole of Y_n^1 for all n. Take $n = n_1 = 1$. If all Y_n^1, $n \geq 2$, contain Y_1^2 in one of their holes then we are in case (ii). Thus we may assume there is some $n_2 > n_1$ such that $Y_{n_2}^1$ is contained in a hole of $Y_{n_1}^2$. Observe that $Y_{n_2}^2$ is contained in a hole of $Y_{n_2}^1$. If all Y_n^1 with $n > n_2$ contain $Y_{n_2}^2$ in one of their holes, we are again in case (ii). Otherwise there is some $n_3 > n_3$ such that $Y_{n_3}^1$ is contained in a hole of $Y_{n_2}^2$. Proceeding in this way we shall find a subsequence of Y_n^1 and of Y_n^2 such that either (ii) or (iii) hold.

The case where both chains are increasing can be analyzed with the same arguments as above.

Suppose that case (i) happens. Then there are two disjoint saturated sets A, B such that $Y_n^1 \subseteq A$, $Y_n^2 \subseteq B$. If the chains Y_n^1 and Y_n^2 are decreasing (i.e., if $Y_{n+1}^i \subseteq sat(Y_n^i)$ for all n) or one is increasing (Y_n^i is increasing if $Y_n^i \subseteq sat(Y_{n+1}^i)$ for all n) while the other is decreasing, then we conclude that the sets Y^1 and Y^2 would be separated by one of the sets Y_n^i and then could not be connected inside X, a contradiction. Thus, both chains Y_n^1, Y_n^2 are increasing. In this case, since Y_n^1 is contained in a hole of Y_{n+1}^1, we cannot connect Y_n^1 to Y_n^2 without crossing Y_{n+1}^1 which is at level μ_{n+1}. Hence, Z_n^1 and Z_n^2 cannot be connected without crossing level μ_{n+1}. We have that $Z_n^1 \neq Z_n^2$ and our conclusion follows.

Suppose that case (ii) happens. Without loss of generality we may assume that the Y_n^1 are inside holes of the Y_n^2, i.e., there is a saturated set H such that the chain $Y_n^1 \subseteq H$ and $H \subseteq sat(Y_n^2)$ for all n. If Y_n^1 is decreasing, then Y^1 and Y^2 would be separated by one of the sets Y_n^1, and could not be connected inside X, a contradiction. If Y_n^1 is increasing, then to connect Y_n^1 to Y_n^2 we cross Y_{n+1}^1 which is at level μ_{n+1}. Then we have that $Z_n^1 \neq Z_n^2$, since to connect both sets we would need to cross level μ_{n+1}.

Suppose that (iii) happens. We may assume that Y_n^1 and Y_n^2 are monotone, either increasing or decreasing. If one of them is increasing and the other is decreasing we would be in case (ii). Thus we may assume that both families are increasing or decreasing. Suppose that both are increasing. For simplicity we shall say that two sets are ordered if one of them is contained in a hole of the other. We know that Y_1^1 and Y_1^2 are ordered. Set $n_1 = 1$. Choosing n_2 sufficiently large, we may assume that $Y_{n_2}^1, Y_{n_2}^2$ are ordered and contain $Y_{n_1}^1, Y_{n_1}^2$ in one of their holes. In this way we construct a subsequence n_j such that $Y_{n_j}^1, Y_{n_j}^2$ are ordered and contained in a hole of each of the ordered pair of sets $Y_{n_{j+1}}^1, Y_{n_{j+1}}^2$ for all j. By extracting a subsequence, if necessary, we may assume that $Y_{n_j}^1$ is contained in a hole of $Y_{n_j}^2$ and both are contained in a hole of $Y_{n_{j+1}}^1$ for all j (or the same relations with 1 and 2 interchanged). Since each set between $Y_{n_j}^1$ and $Y_{n_j}^2$ has area $\geq \delta$, this would represent an infinite area in the intertwined chain. The same conclusion would follow in case that both chains are decreasing.

In any case, we conclude that there is a sequence of n's such that $Z_n^1 \neq Z_n^2$, hence $sig([u \geq \lambda]) \neq sig([u \geq \mu_n])$, and, therefore, λ is a critical value of u.

Finally, we assume that $\eta_-(x, \lambda) = \lambda$. Then there is $X \in \mathcal{CC}([u = \lambda])$ such that $X_\epsilon := \mathcal{CC}([\lambda - \epsilon \leq u \leq \lambda], X)$ is not a monotone section for any $\epsilon > 0$. Since $\cap_{\epsilon > 0} X_\epsilon = X$, for $\epsilon > 0$ small enough we have that the only connected component of $[u = \lambda]$ contained in X_ϵ is X. Take such an ϵ. By Proposition 1, we find a sequence $\mu_n \uparrow \lambda$ such that $X_\epsilon \cap [u = \mu_n]$ are not connected. Let Y_n^1, Y_n^2 be two connected components of $X_\epsilon \cap [u = \mu_n]$. Observe that $Y_n^1, Y_n^2 \subseteq X_\epsilon \cap [u = \mu_n] \subseteq X$.

By changing $u \to -u$ and repeating the argument above we conclude that the sets $Z_n^1 = \mathcal{CC}([u \leq$

$\mu_n], Y_n^1)$ and $Z_n^2 = \mathcal{CC}([u \leq \mu_n], Y_n^2)$ are different connected components of $[u \leq \mu_n]$. Since

$$\mathcal{CC}([u \leq \mu_n], Y_n^1) = \cap_{\mu > \mu_n} \mathcal{CC}([u < \mu], Y_n^1)$$

$$\mathcal{CC}([u \leq \mu_n], Y_n^2) = \cap_{\mu > \mu_n} \mathcal{CC}([u < \mu], Y_n^2)$$

if there is a sequence $\mu_n^k \downarrow \mu_n$ such that

$$\mathcal{CC}([u < \mu_n^k], Y_n^1) = \mathcal{CC}([u < \mu_n^k], Y_n^2),$$

we would obtain that

$$Z_n^1 = \mathcal{CC}([u \leq \mu_n], Y_n^1) = \mathcal{CC}([u \leq \mu_n], Y_n^2) = Z_n^2,$$

a contradiction. Thus, for each n, there is an $\epsilon_n > 0$ such that

$$\mathcal{CC}([u < \mu], Y_n^1) \neq \mathcal{CC}([u < \mu], Y_n^2),$$

for all $\mu \in (\mu_n, \mu_n + \epsilon_n)$. Thus we find a sequence $\mu_n' \uparrow \lambda$ such that

$$\mathcal{CC}([u < \mu_n'], Y_n^1) \neq \mathcal{CC}([u < \mu_n'], Y_n^2), \tag{5}$$

for all n. Let $\lambda' > \lambda$. Let $Z = \mathcal{CC}([u < \lambda'], X)$. Observe that $Y_n^1, Y_n^2 \subseteq X \subseteq Z$, hence $Z_n^1, Z_n^2 \subseteq Z$. Then (5) implies that $sig([u \geq \mu_n'], [u < \mu_n']) \neq sig([u \geq \lambda'], [u < \lambda'])$. Since the signature is locally constant at the left of λ, we conclude that $sig([u \geq \lambda], [u < \lambda]) = sig([u \geq \mu_n'], [u < \mu_n']) \neq sig([u \geq \lambda'], [u < \lambda'])$, and this holds for all $\lambda' > \lambda$, i.e., λ is a critical value of u. □

Remark 6 From Remark 5 and the above results it follows that λ is a critical value of u if and only if $-\lambda$ is a critical value of $-u$.

The developments of this Section permit us to compute the singular values of the topographic map of u by computing the critical values of u. Moreover, at the discrete level, a topological change occurs when going from level λ to level $\lambda - 1$ if and only if either $i)$ $sig([u \geq \lambda]) \neq sig([u \geq \lambda - 1])$, or $ii)$ $sig([u < \lambda]) \neq sig([u < \lambda - 1])$. This is equivalent to saying that $i)$ two connected components of $[u \geq \lambda]$ merged at level $\lambda - 1$, a phenomenon which we call merging of upper connected components, or a new connected component of the upper level sets was born at level $\lambda - 1$, or $ii)$ two connected components of $[u < \lambda - 1]$ merged at level λ, a phenomenon which we call merging of lower connected components, or a new connected component of the lower level sets was born at level λ (see Fig. 9). We call the first type of criticality of upper type, while the second is called of lower type.

6.1 The computational algorithm

For the sake of simplicity we only describe the algorithm to compute the critical values of upper type. The critical values of lower type can be computed using the same algorithm applied to the inverted image $\max(u) - u$. Note that it is possible to compute both types of criticalities at the same time. Anyway, the computational cost will be similar either if we compute the $\sup$ and $\inf$ monotone sections separately or at the same time. As we will see in Algorithm 1, the computational cost derives mainly from the computation of the connected components at each level. Since we perform this computation by means of a region growing strategy, it makes no difference to do both computations (upper and lower connected components) simultaneously or not.

Let D be an interval of $\mathbb{R}^2$ and $u : D \to \mathbb{R}$ a continuous function. To simplify our terminology we call sup-monotone section a connected component X of an upper level set $[u \geq \lambda]$ which contains no criticalities

of upper type due to merging of connected components of upper level sets. Note that it contains a single critical value due to the birth of the connected component corresponding to a zonal maximum. As already mentioned, for simplicity we only describe how to compute the sup-monotone sections. The corresponding inf-monotone sections can be computed with the same algorithm applied to $max(u) - u$.

We have observed that due to low oscillations in the image, a large number of criticalities may appear. In order to avoid this problem we have used two different strategies. The first one consists on making a pre-filtering step to reduce the number of low oscillations present in the image.[3] This pre-filtering step can be done by means of the extrema filters which preserves as much as possible the topographic map structure [8, 14]. The second strategy (which can be combined or not with the pre-filtering step) consists on discarding those critical sections which do not satisfy a minimum contrast criterion, in other words, low contrasted sup-monotone sections will be discarded. The contrast criteria is specified by means of a parameter $MinContrast$.

We need some additional simple notation in order to make explicit an algorithm taking into account the contrast criterion. Denote by $(X^{\lambda,p_i}, \beta^{\lambda,p_i})$ the sup-monotone section of $[u \geq \lambda]$ beginning in β^{λ,p_i}, thus it contains no criticality of upper type due to merging. We can define now a measure of contrast C for the couple $(X^{\lambda,p_i}, \beta^{\lambda,p_i})$ simply by $C(X^{\lambda,p_i}, \beta^{\lambda,p_i}) = \beta^{\lambda,p_i} - \lambda$. Note that at a critical level μ the couple $(X^{\mu,p_i}, \beta^{\mu,p_i})$ defines a maximal sup-monotone section of the topographic map starting at level β^{μ,p_i} and ending at level μ (see Fig. 3).

We assume that our image u ranges from $m = min(u)$ to $M = max(u)$ (for example from 0 to 255). To store the computed connected components we use a dynamical data structure L consisting on a vector, ranging from m to M, of lists of couples $(X^{\lambda,p_i}, \beta^{\lambda,p_i})$. The algorithm computing the maximal sup-monotone sections is summarized in Table 1.

It is important to remark that the parameter $MinContrast$ allows us to discard low contrasted sup-monotone sections in a *causal* way. That is, if we denote as $MS(u, MinContrast)$ the set of maximal sup-monotone sections of u with contrast $\geq MinContrast$, then the inclusion principle $MS(u, 0) \supset MS(u, 1) \supset \ldots \supset MS(u, n)$ holds. An example of the performance of the preceding algorithm is presented in Fig. 11, where we have computed the critical sections of a low resolution synthetic image.

As we noted in the Introduction, many different approaches exist to compute the basic Morse structure of images or 3D data. We have presented a simple computational approach and have studied its mathematical properties. Let us note that the singularities of the tree of shapes of an image as introduced in [38], [9], coincide with the notion of critical value defined here [15].

7 Drainage structure

In the previous section we have developed an algorithm to compute the Morse structure of an image. This Morse structure consists on the maxima, minima, and the level lines where a topology change occurs (i.e., the boundaries of the maximal monotone sections). This can be considered as a reasonable *global* description of a DEM. But, it is not sufficient to encode Digital Elevation Models (DEM). There are also other structures which are of special interest due to its topographic significance in DEM data. These structures correspond mainly to the drainage structures (e.g., rivers and ravines). There exists many different algorithms accurately computing such structures, see [34] and references therein. Since the accurate computation of the drainage patterns in a DEM is computationally expensive we shall compute a good approximation to these structures. We will present an approach which is related to the one in [55]. This section describes and justifies a morphological approach to compute such approximation. Strictly speaking, we do not compute the drainage

[3] Note that this filtering is done only for the computation of the Morse structure. All other operations, and in particular the maximal encoding error, refer to the original image.

Algorithm 1

1 *Set $\lambda = M$ and compute X^{λ,p_i} and set $\beta^{\lambda,p_i} = M$, $\forall i$.*

2 *Store the couples $(X^{\lambda,p_i}, \beta^{\lambda,p_i})$ in $L[\lambda]$.*

3 *If $(\lambda - 1) > m$, set $\lambda = \lambda - 1$, and recompute X^{λ,p_i}(note the abuse of notation on λ and p_i); else go to step **8**.*

4 *$\forall p_i \in sig([u \geq \lambda])$ if $p_i \in sig([u \geq \lambda + 1])$ and X^{λ,p_i} was not marked as critical, then $\beta^{\lambda,p_i} = \beta^{\lambda+1,p_i}$; else $\beta^{\lambda,p_i} = \lambda$*

5 *Let $A = sig([u \geq \lambda + 1]) \backslash (sig([u \geq \lambda + 1]) \cap sig([u \geq \lambda]))$.*

6 *If $A \neq \phi$ then $\forall p \in A$ search $q \in sig([u \geq \lambda])$ such that $p \in X^{\lambda,q}$ and mark $X^{\lambda,q}$ as critical.*

7 *Return to step **2**.*

8 *Select from L the list of couples $(X^{\lambda,p}, \beta^{\lambda,p})$ marked as critical and verifying that $C(X^{\lambda,p}, \beta^{\lambda,p}) \geq MinContrast$.*

9 *The output of the algorithm will be the set of curves Γ_M corresponding to the boundaries of the selected sections $X^{\lambda,p}$ and its markers.*

Table 1: Algorithm for computing the maximal sup-monotone sections of an image.

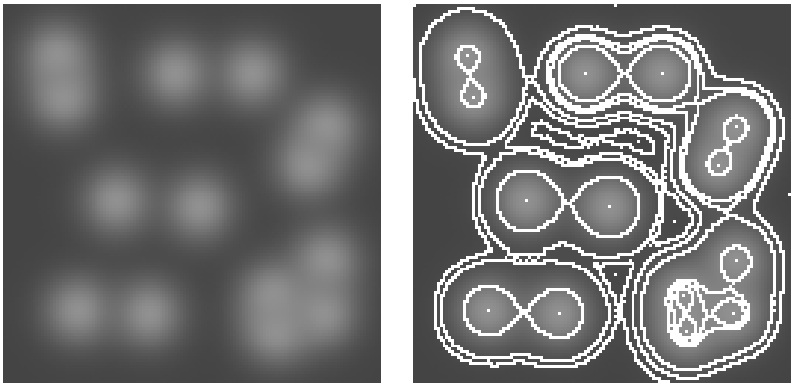

Figure 11: Left: synthetic image representing a set of peaks. Right: Computed saddle structures and criticalities.

structures but a version of them which is adapted to our purposes. The algorithm computing these structures will be detailed in Section 8.

Let $u : [0,1] \times [0,1] \to I\!R$ be a continuous function. Let Let $\epsilon > 0$. For each $y \in [0,1]$ we define the

filtered images

$$SI^{\epsilon,1d}u(.,y)(x)$$

$$IS_{\epsilon,1d}u(.,y)(x)$$

For simplicity, we shall denote them by $SI^{\epsilon,1d}u(x,y)$, $IS_{\epsilon,1d}u(x,y)$.

Lemma 11 *The functions $SI^{\epsilon,1d}u(x,y)$, $IS_{\epsilon,1d}u(x,y)$ are continuous in $[0,1]\times[0,1]$.*

Proof: Both cases being similar, we shall only consider the case of the operator $SI^{\epsilon,1d}$. Let $y_n \to y \in [0,1]$ and let $u_n(x) = u(x,y_n)$. Then, by Proposition 4, we have that $SI^{\epsilon,1d}u_n \to SI^{\epsilon,1d}u(.,y)$ uniformly as $n\to\infty$. We deduce that for each fixed value of y, $SI^{\epsilon,1d}u(.,y)$ is a continuous function of x.

Let $(x,y)\in[0,1]\times[0,1]$ and let $(x_n,y_n)\to(x,y)$. Since $SI^{\epsilon,1d}u_n \to SI^{\epsilon,1d}u(.,y)$ uniformly as $n\to\infty$, given $\delta>0$, let n_0 be large enough so that

$$|SI^{\epsilon,1d}u_n(x) - SI^{\epsilon,1d}u(x,y)| \le \delta$$

for all $n\ge n_0$ and all $x\in[0,1]$. Then, for $n\ge n_0$,

$$\begin{aligned} |SI^{\epsilon,1d}u(x_n,y_n) - SI^{\epsilon,1d}u(x,y)| &\le |SI^{\epsilon,1d}u(x_n,y_n) - SI^{\epsilon,1d}u(x_n,y)| \\ &+ |SI^{\epsilon,1d}u(x_n,y) - SI^{\epsilon,1d}u(x,y)| \\ &\le \delta + |SI^{\epsilon,1d}u(x_n,y) - SI^{\epsilon,1d}u(x,y)|. \end{aligned}$$

If we take $\limsup$, we obtain

$$\begin{aligned} &\limsup_n |SI^{\epsilon,1d}u(x_n,y_n) - SI^{\epsilon,1d}u(x,y)| \le \\ &\delta + \limsup_n |SI^{\epsilon,1d}u(x_n,y) - SI^{\epsilon,1d}u(x,y)| = \delta, \end{aligned}$$

since $SI^{\epsilon,1d}u(.,y)$ is a continuous function of x. Since the above inequality is true for all δ we conclude that $SI^{\epsilon,1d}u(x_n,y_n)\to SI^{\epsilon,1d}u(x,y)$ as $n\to\infty$. Therefore, $SI^{\epsilon,1d}u(x,y)$ is continuous. □

Let $U_\epsilon(x,y) = IS_{\epsilon,1d}SI^{\epsilon,1d}u(x,y)$. By the above Lemma, U_ϵ is a continuous function.

Definition 9 *Let $f:[0,1]\to I\!R$ be a continuous function. We say that $x_0\in[0,1]$ is a zonal maximum (minimum) of f if there is an interval $I_{x_0}=[x_1,x_2]$ containing x_0 such that $f(x)=f(x_0)$ for all $x\in I_{x_0}$ and there is some $\delta>0$ such that $f(x)<f(x_0)$ (resp. $f(x)>f(x_0)$) for all $x\in((x_1-\delta,x_1)\cup(x_2,x_2+\delta))\cap[0,1]$.*

Lemma 12 *For each $y\in[0,1]$, the function $U_\epsilon(.,y)$ has a finite number of zonal maxima and minima. Indeed the total number of zonal maxima and minima is bounded by $\frac{1}{\epsilon}$.*

Proof: Let $y\in[0,1]$ be fixed. We observe that if x_0 is a zonal maximum (minimum) of $U_\epsilon(.,y)$ then the associated interval I_{x_0} contains $\mathcal{CC}([U_\epsilon(.,y)\ge U_\epsilon(x_0,y)],x_0)$ (resp. $\mathcal{CC}([U_\epsilon(.,y)\le U_\epsilon(x_0,y)],x_0)$) and this has length $\ge\epsilon$. Thus, if $x_1,x_2,...,x_p$ are different zonal maxima or minima corresponding to disjoint intervals then $p\epsilon\le 1$. Hence, their number is bounded by $\frac{1}{\epsilon}$. □

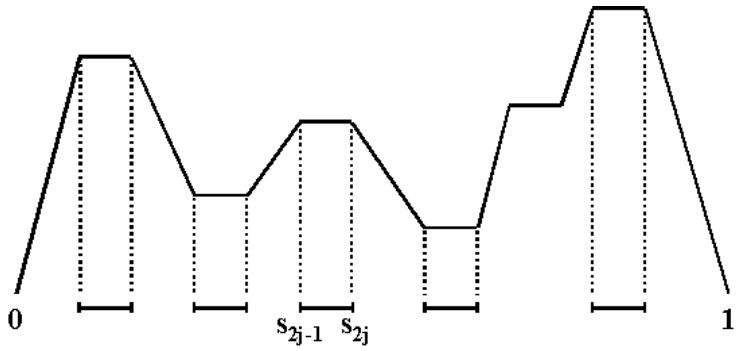

Figure 12: The intervals containing the extrema of a $1D$ signal.

The above Lemma gives a description of the function U_ϵ as functions of x for each fixed $y \in [0,1]$. These functions have a finite number of zonal extrema, either maxima or minima, there is a zonal minimum (maximum) between two consecutive maxima (minima) and the rest is made of monotone pieces. For each fixed $y \in [0,1]$ let $I_1(y), ..., I_p(y)$ (where $p = p(y)$) be the intervals corresponding to the zonal maxima and minima. By the above remarks, we have that $p = p(y) \leq \frac{1}{\epsilon}$. They are closed intervals of length at least ϵ and we denote them by $I_j(y) = [s_{2j-1}(y), s_{2j}(y)]$, $j = 1, ..., p$ (see Fig. 12). We are going to encode the points $\mathcal{S} := \{(s_j(y), y) : j = 1, ..., 2p(y),\ y \in [0,1]\}$. Our purpose is to prove that these points are contained in a family of graphs of Borel functions of y.

Proposition 9 *The family of points $\mathcal{S}$ is contained in a (at most, countable) family of graphs of Borel functions of y.*

Proof: Let q_n be an enumeration of the rational points of $(0, \epsilon)$. Let $\mathcal{T}$ be the set of points $(x, y) \in [0,1] \times [0,1]$ such that either

$$U_\epsilon(x - \frac{1}{m}, y) < U_\epsilon(x, y) = U_\epsilon(x + q_n, y) \quad \forall\, m \geq m_0, \text{ and some } m_0, \text{ and all } n,$$

or

$$U_\epsilon(x - \frac{1}{m}, y) > U_\epsilon(x, y) = U_\epsilon(x + q_n, y) \quad \forall\, m \geq m_0, \text{ and some } m_0, \text{ and all } n,$$

or

$$U_\epsilon(x + \frac{1}{m}, y) < U_\epsilon(x, y) = U_\epsilon(x - q_n, y) \quad \forall\, m \geq m_0, \text{ and some } m_0, \text{ and all } n,$$

or

$$U_\epsilon(x + \frac{1}{m}, y) > U_\epsilon(x, y) = U_\epsilon(x - q_n, y) \quad \forall\, m \geq m_0, \text{ and some } m_0, \text{ and all } n.$$

Observe that $\mathcal{S} \subseteq \mathcal{T}$. Since the sets of points $\{(x,y) : U_\epsilon(x \pm \frac{1}{m}, y) < U_\epsilon(x,y)\}$, $\{(x,y) : U_\epsilon(x \pm \frac{1}{m}, y) > U_\epsilon(x,y)\}$ are open and the sets $\{(x,y) : U_\epsilon(x \pm q_n, y) = U_\epsilon(x,y)\}$, $\{(x,y) : U_\epsilon(x \pm q_n, y) = U_\epsilon(x,y)\}$ are closed, we conclude that the set $\mathcal{T}$ is a Borel set. Moreover, since for each $y \in [0,1]$ the set $\mathcal{T}_y = \{x \in [0,1] : (x,y) \in \mathcal{T}\}$ is finite, by Lusin's Theorem [59], Theorem 5.8.11, we conclude that $\mathcal{T}$ is contained in a (at most, countable) family of Borel graphs of functions of y. Therefore, also is $\mathcal{S}$. □

8 Computing the drainage structure

In a simplistic way we can think of the drainage structures as the set of points for which there exists at least one direction in which the flow of water is accumulated or repealed. We can write down this definition

mathematically by considering the set of points $\{\vec{x} : \exists \vec{v} \in I\!R^2$ and $\varepsilon \geq 0$ such that $u(\vec{x}) \leq u(\vec{x} + t\vec{v})$ $\forall t \in (-\varepsilon, \varepsilon)$, or $u(\vec{x}) \geq u(\vec{x} + t\vec{v})$ $\forall t \in (-\varepsilon, \varepsilon)\}$. Observe that this set of points will contain in particular the maxima and minima of u. It has been shown in Section 7 that this set of points is contained in an at most a countable family of Borel curves. Intuitively, these curves contain the drainage structures (ridges and valleys), giving also information about boundaries of plateaus for example. In the discrete case we only consider 4 different directions (values of v) corresponding to 4 different profiles in the image. Concretely, we search maxima and minima of the vertical, horizontal and diagonal profiles. In [55] only two directions were used, namely the horizontal and vertical ones.

Algorithm 2

1 *Set* $(v1, p1) \leftarrow ComputeExtrema(x)$

2 *Set* $v^f = v1$

3 *for* $j = 1$ *to* $length(v1)$ *do*
compute $c_{left} = |v(j) - v(j-1)|$
compute $c_{right} = |v(j) - v(j+1)|$
if $c_{left} < thr$ *or* $c_{right} < thr$ *then*
set $c_{left} = |v^f(j) - v^f(j-1)|$
if $c_{left} < thr$ *then*
$v^f(j) = v^f(j-1)$
else
$v^f(j) = v^f(j+1)$
end if
end if
end for

4 *Set* $(v2, p2) \leftarrow ComputeExtrema(v^f)$

5 *Set* $p(i) = p1(p2(i))$ $\forall i = 1 .. length(p2)$. *This vector* p *contains the* x *coordinates of the selected extrema. We can think of* p *as the vector defining the intervals of monotonicity of* x *after the filtering. Due to the flatness of* v^f*, in each interval* $(p(i-1), p(i+1))$ *the extrema* $v2(p(i))$ *could not be the absolute maximum (minimum) so we have to recompute it in each of these intervals.*

6 *Finally, if an extrema* $v2(i)$ *lies in a flat zone we redefine the extrema as the boundaries of this flat zone.*

Table 2: Algorithm for computing the significant extrema of a $1D$ profile.

In order to specify the algorithm we assume that we have a simple subroutine, *ComputeExtrema*, which receives as input a vector $x = [x(1), ..., x(n)]$ and returns two vectors (v, p), where $v = [v(1), ..., v(k)]$ contains the maxima and minima of x consecutively and $p = [p(1), ..., p(k)]$ its relative positions in such a way that $v(i) = x(p(i))$. The problem is that a large number of extrema can appear due to low oscillations,

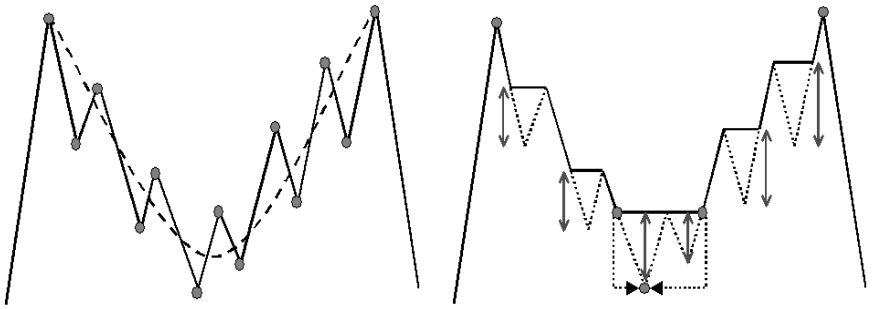

Figure 13: Left: computed maxima and minima of a 1D signal. The dotted curve denotes the ideal profile (before introducing electronic and quantization noise which is always present in digital images). Right: signal obtained by filtering the less contrasted extrema according to **Algorithm 2** (light gray arrows depict the contrast of the filtered extrema). Note that if we simply reject those extrema instead of filtering them with **Algorithm 2**, then the only computed extrema would be the two maxima.

mainly due to noise. In order to solve this problem we have to choose the most significant extrema, in our case those which have maximum *contrast*. The contrast of an extremum $v(i)$ can be defined simply by $C(v(i)) = min(|v(i) - v(i-1)|, |v(i) - v(i+1)|)$. Using this criteria directly, for example by eliminating those extrema with contrast less than a threshold thr, produces undesirable results (see Fig. 13). Instead of using the contrast to eliminate extrema points we use it to filter them. The filtering step simply consists on replacing the value of $v(i)$ by $v(i-1)$ if $C(v(i)) = |v(i) - v(i-1)| < thr$ or $v(i+1)$ if $C(v(i)) = |v(i) - v(i+1)| < thr$. These filtering step produces a new vector v^f and recomputing the extrema of v^f produces a more desirable result, see Fig. 13. If any computed extremum lie in a flat zone (i.e., it is a zonal extremum), we shall replace it by the boundary of the flat zone. The algorithm computing these significant extrema from a 1D-profile x is summarized in table 2.

Figure 13 illustrates the extrema filtering process. On the left we show the real (solid line) and the ideal (dotted line) profile without noise and its extrema. On the right we show the profile after the filtering process. Note that the filtered profile contains a new minimum (zonal minimum in fact) which does not coincide with any of the minima of the original signal. This is solved easily by recomputing the absolute minimum in the interval where the filtered signal is convex (see step **5** of **Algorithm 2**).

Figure 14 shows the output of the algorithm just presented using a real profile of DEM data. In order to obtain the desired curves we must compute the maxima and minima of all the selected profiles of the image. As we have previously said, we compute these curves using the horizontal, vertical and diagonal profiles of the image.

Figure 15 illustrates the whole geometric sampling process. From left to right and top to bottom we show the original DEM image, the level lines Γ_M corresponding to its Morse structure ($MinContrast = 10$), the curves Γ_D corresponding to the extrema of the profiles ($thr = 10$), and the final sampling $\Gamma_{xy} = \Gamma_M \cup \Gamma_D$. A thinning step has been performed in order to obtain one pixel width curves.

9 Interpolation

As we have explained in the above sections, given the elevation data $u(x, y)$, the samples we take on u are based on the level lines at the critical levels of u and a morphological sampling which tries to approximate the ridges and ravines of u. At the continuous level the critical level lines are computed on a filtered version of u so that, by Theorem 1, there are only a finite number of them. Under mild assumptions on u (for instance, the level sets of u are rectifable) the level curves at the critical levels of u constitute a family of

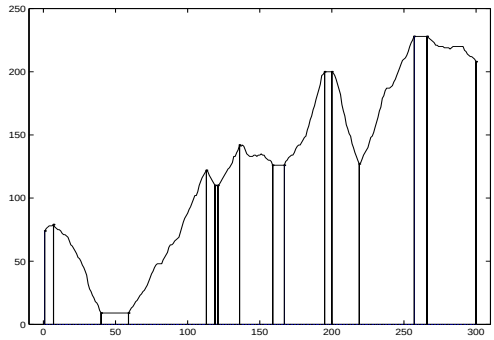

Figure 14: Computed zonal maxima and minima of one image profile using the algorithm described above with a contrast parameter of 10.

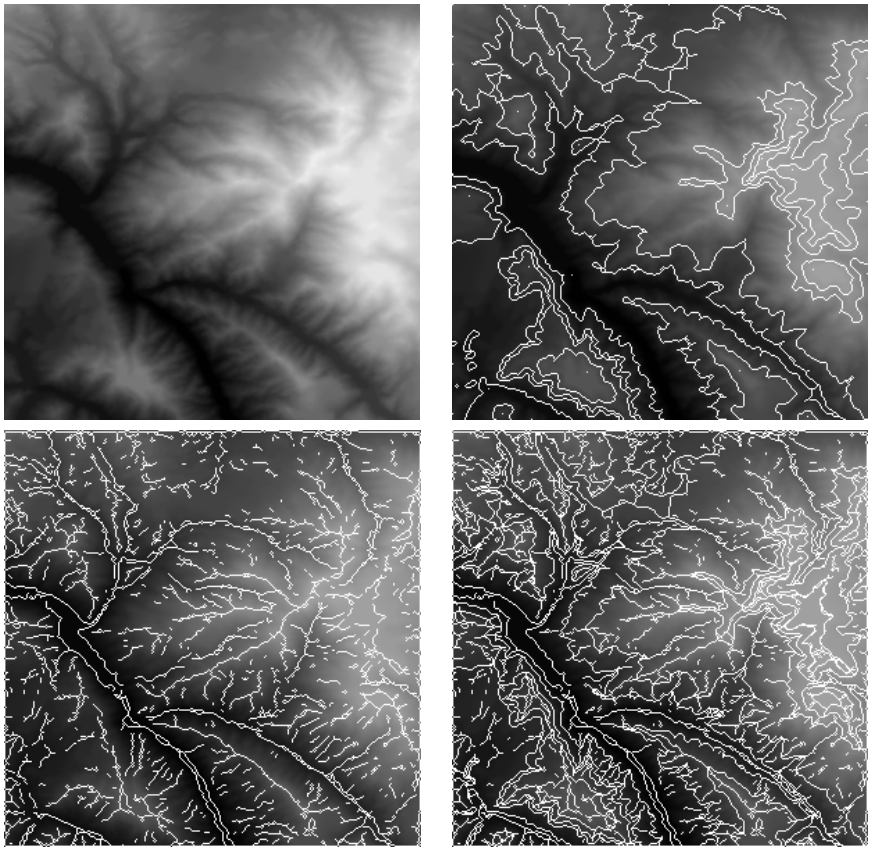

Figure 15: From left to right and up to down: the original DEM image, computed level lines (white), computed ridge/valley structure (white) and the whole image sampling (white).

Jordan curves bounding open regions. The zonal extrema are regions of area $\geq \delta$, $\delta > 0$ being the area threshold used for the grain filter. The rest of the sample points are organized as a series of curves and eventually isolated points.

In this section we will discuss some interpolation methods used to recover an approximation of u from its samples, specially the Laplacian and the AMLE model. In a general framework (introduced in [16]) we will prove that under some assumptions the interpolation methods based on PDE's can be considered as

shape preserving methods. Since the Laplace operator is well-known, we shall only state the basic results required for the AMLE model. In particular, we study some bounds on the error for the AMLE model.

Let Ω be a bounded connected domain in $\mathbb{R}^N$. Given Ω, let $d_\Omega : \overline{\Omega} \times \overline{\Omega} \to \mathbb{R}$ be the distance metric relative to Ω, i.e.,

$$d_\Omega(x,y) = \liminf_{(\xi,\eta)\to(x,y)} \left(\inf \left\{ \int_0^1 |\frac{d\zeta}{dt}|\, dt : \zeta \in \mathcal{W} \right\} \right)$$

where $\mathcal{W} := \{\zeta \in C^1([0,1],\Omega), \zeta(0) = \xi,\ \zeta(1) = \eta\}$. $d_\Omega(x,y)$ is the geodesic distance between x and y, i.e., the minimal length of all possible paths joining x and y and contained in Ω [25].

We define $Lip_\partial(\Omega)$ by

$$Lip_\partial(\Omega) = \{g \in C(\partial\Omega) : |||g||| = \sup_{x,y\in\partial\Omega} \frac{|g(x)-g(y)|}{d_{\partial\Omega}(x,y)} < \infty\}.$$

If $\partial\Omega$ is smooth, then $Lip_\partial(\Omega) = W^{1,\infty}(\partial\Omega)$ but $Lip_\partial(\Omega)$ is defined for more general domains. If $g \in Lip_\partial(\Omega)$ then the functions

$$g^+(x) = \inf_{y\in\partial\Omega} (g(y) + |||g|||d_\Omega(x,y))$$

$$g^-(x) = \sup_{y\in\partial\Omega} (g(y) - |||g|||d_\Omega(x,y))$$

are minimal Lipschitz extension of g into Ω, i.e., $u \in W^{1,\infty}(\Omega) \cap C(\overline{\Omega})$, $g^\pm|_{\partial\Omega} = g$ and

$$\| Dg^\pm \|_{L^\infty(\Omega,\mathbb{R}^N)} \leq \| Dw \|_{L^\infty(\Omega,\mathbb{R}^N)}$$

for all w with $w - g^\pm \in W_0^{1,\infty}(\Omega)$ ([25], Theorem 1.8 and [3]).

The minimal Lipschitz extensions are not unique [3], [25]. In [3], Aronsson studied the Lipschitz extensions which are obtained as limits when $p \to \infty$ of the so called minimal p-extensions, i.e., functions u such that

$$\| Du \|_{L^p(\Omega,\mathbb{R}^N)} \leq \| Dw \|_{L^p(\Omega,\mathbb{R}^N)}$$

for all w such that $w - u \in W_0^{1,p}(\Omega)$. For minimal p-extensions the above condition is equivalent to

$$\| Du \|_{L^p(\Omega',\mathbb{R}^N)} \leq \| Dw \|_{L^p(\Omega',\mathbb{R}^N)}$$

for all $\Omega' \subseteq \Omega$ and all w such that $w-u \in W_0^{1,p}(\Omega')$. Passing to the limit in the above inequalities, Aronsson [3, 4] defined an $AMLE$ as a function $u \in W^{1,\infty}(\Omega) \cap C(\overline{\Omega})$ such that

$$\|Du\|_{L^\infty(\Omega';\mathbb{R}^N)} \leq \|Dw\|_{L^\infty(\Omega';\mathbb{R}^N)} \tag{6}$$

for all $\Omega' \subseteq \Omega$ and w such that $u - w \in W_0^{1,\infty}(\Omega')$. Moreover, Aronsson proved that for smooth $AMLE$'s the Euler equation of (6) is

$$D^2u\,(Du, Du) = 0 \quad \text{in } \Omega. \tag{7}$$

Later, Jensen [25] proved the uniqueness of the $AMLE$ extension of $\varphi \in Lip_\partial(\Omega)$ and he characterized it as the unique viscosity solution of (7) with boundary data

$$u_{|\partial\Omega} = \varphi. \tag{8}$$

Given $u \in C(\Omega)$ we say that u is a viscosity subsolution (supersolution) of (7) if for any $\psi \in C^2(\Omega)$ and any x_0 local maximum (minimum) of $u - \psi$ in Ω

$$D^2\psi(x_0)(D\psi(x_0), D\psi(x_0)) \geq 0 \quad (\leq 0).$$

A viscosity solution is a function which is a viscosity sub- and supersolution. Then Jensen proved [25] a comparison principle between sub- and supersolutions of Equation (7) together with an existence result for boundary data in $Lip_\partial(\Omega)$.

Theorem 2 *Assume that v is a viscosity subsolution and w a viscosity supersolution of (7). If $v\mid_{\partial\Omega}$, $w\mid_{\partial\Omega} \in Lip_\partial(\Omega)$ then*

$$\sup_{x\in\Omega}(v-w) = \sup_{x\in\partial\Omega}(v-w) \tag{9}$$

Theorem 3 *Given $g \in Lip_\partial(\Omega)$, u is the $AMLE$ of g into Ω if and only if u is the viscosity solution of (7) with $u\mid_{\partial\Omega} = g$.*

The following existence result for (7) follows from R. Jensen's results.

Theorem 4 *Given $g \in Lip_\partial(\Omega)$, then there exists a unique viscosity solution $u \in W^{1,\infty}(\Omega)$ of (7) such that $u\mid_{\partial\Omega} = g$. Moreover $\| Du \|_{L^\infty(\Omega,\mathbb{R}^N)} = |||g|_{\partial\Omega}|||$.*

He further extended the comparison principle 9, and Theorems 3, 4 to the case of continuous boundary data $g \in C(\partial\Omega)$ and proved that in that case, the $AMLE$ is locally Lipschitz continuous in Ω [25].

An important result proved by Aronsson in [4] was that smooth $AMLE$ do not have critical points inside Ω. More precisely, he proved:

Theorem 5 *Let $\Omega \subseteq \mathbb{R}^2$ and $u \in C^2(\Omega)$ be a nonconstant solution of (7). Then $|Du| > 0$ in Ω.*

Moreover, in [5] he gave examples of C^1 non-constant (viscosity) solutions of (7) having an interior critical point. Let us mention that such result has also been proved (in any dimension) for starshaped annulus and capacitary boundary data by E. Rosset [46]. In next Theorem we remark that a weaker but related result holds. We shall write it in a more general context.

Following [16], we shall consider an interpolation operator as a transformation E which associates to each open bounded set Ω and each function $\varphi \in C(\partial\Omega)$ a function $E(\varphi,\Omega) \in C(\overline{\Omega})$ such that $E(\varphi,\Omega)|_{\partial\Omega} = \varphi$. We shall say that the interpolation operator satisfies the stability principle if

$$E(E(\varphi,\Omega)|_{\partial\Omega'},\Omega') = E(\varphi,\Omega)|_{\Omega'}$$

for any open bounded set Ω, any $\varphi \in \partial\Omega$, and any open bounded set $\Omega' \subseteq \Omega$. Suppose that the interpolation operator E satisfies the stability property, we say that E satisfies the maximum principle if

$$\inf_{\partial\Omega'}\varphi \le \inf_{\overline{\Omega'}} E(\varphi,\Omega') \le \sup_{\overline{\Omega'}} E(\varphi,\Omega') \le \sup_{\partial\Omega'}\varphi \tag{10}$$

for any open bounded set Ω, any open bounded set $\Omega' \subseteq \Omega$, and any $\varphi \in C(\partial\Omega')$. If E satisfies the maximum principle and $\varphi = \alpha$ in $\partial\Omega$, where $\alpha \in \mathbb{R}$, then $E(\varphi,\Omega) = \alpha$ in $\overline{\Omega}$, and the same is true in any open bounded set $\Omega' \subseteq \Omega$.

Theorem 6 *Let Ω_2 be an open simply connected set. Let Ω_1 be an open set whose boundary $\partial\Omega_1$ is connected and $\overline{\Omega_1} \subseteq \Omega_2$. Let $\Omega = \Omega_2 \setminus \overline{\Omega_1}$. Assume that $u|_{\partial\Omega_1} = \lambda$, $u|_{\partial\Omega_2} = \mu$ with $\lambda < \mu$ or $\lambda > \mu$. Let E be an interpolation operator satisfying the stability and the maximum principle. Then $E(u|_{\partial\Omega},\Omega)$ contains only a monotone section in the sense that $\overline{\Omega}$ is a monotone section of $E(u|_{\partial\Omega},\Omega)$. In particular, if $E(u|_{\partial\Omega},\Omega)$ is the $AMLE$ extension of the boundary data inside Ω, then $E(u|_{\partial\Omega},\Omega)$ contains only a monotone section.*

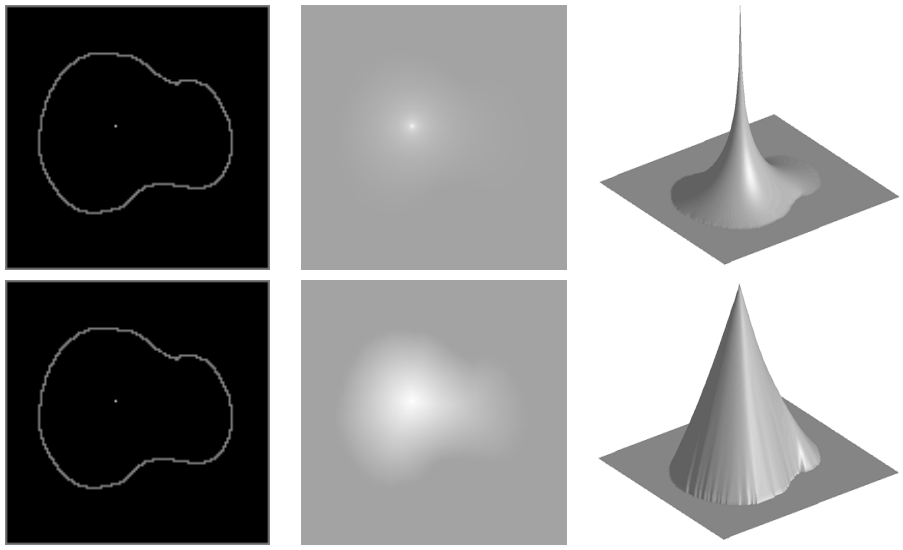

Figure 16: Up: from left to right the initial data, the interpolated data using Laplacian interpolation and its $3D$ representation. Down: from left to right the initial data, the interpolated data using AMLE interpolation and its $3D$ representation.

Proof: To fix ideas, assume that $\lambda > \mu$. First, let us observe that there cannot be interior local minima or maxima. Indeed, if C is an interior zonal minimum at level α, then for some $\delta > 0$ there is a connected component V of $[\alpha \leq u < \alpha + \delta]$ which is an open set containing C whose boundary is contained in $[u = \alpha + \delta]$. Then, since E satisfies the stability and the maximum principles, the interpolation $E(u|_{\partial\Omega}, \Omega)$ inside V, given the boundary data $u = \alpha + \delta$ on ∂V, would be constant and equal to $\alpha + \delta$, a contradiction. Similarly, we prove that there cannot be a local maximum of u in Ω. As a consequence, we conclude that u is monotone. Otherwise, there are levels $\alpha, \beta \in [\lambda, \mu]$ with $\alpha \leq \beta$ such that $[\alpha \leq u \leq \beta]$ is not connected. Let C and D be two connected components of $[\alpha \leq u \leq \beta]$. If the saturations of C and D are disjoint then, by Lemma 5, either $sat(C)$ or $sat(D)$ contains an interior extrema. The same conclusion holds if one of them does not contain $\overline{\Omega_1}$. Thus, without loss of generality we may assume that $\overline{\Omega_1} \subseteq sat(C) \subseteq sat(D)$. Then, using again Lemma 5, there is an extremum inside $sat(D) \setminus sat(C)$, again a contradiction. □

Figure 16 illustrates Theorem 6. In this figure we present the interpolation of the same data using the Laplacian and the AMLE model. First we observe the effect produced by the Laplace interpolation, which is to be expected, since the Laplacian is unable to interpolate with values prescribed on a point. Numerically, the effect is a cusp at the point where the data were prescribed. Observe that since both interpolators satisfy the stability and the maximum principle we obtain no new maxima or minima. Thus, any interpolation operator satisfying the stability and the maximum principle can be considered as a shape preserving interpolator, that is, it will preserve the monotonicity of the data.

Next two Lemmas are auxiliary to prove estimates on the error produced when we have errors on the position of the level curves and errors on the values on it.

Lemma 13 *Let $\Omega_1 \subseteq \Omega_2$ be two open connected domains and let $\varphi_i \in Lip_\partial(\Omega_i)$, $i = 1, 2$. Let u_i be the $AMLE$ extension of φ_i to Ω_i, $i = 1, 2$. Then*

$$\sup_{\Omega_1}(u_2 - u_1) \leq \sup_{\partial\Omega_1}(\varphi_2^+ - \varphi_1) \qquad \textit{and} \qquad \sup_{\Omega_1}(u_1 - u_2) \leq \sup_{\partial\Omega_1}(\varphi_1 - \varphi_2^-).$$

Proof: The Lipschitz estimate on u_2 proves that

$$\varphi_2(y) - |||\varphi_2|||d_{\Omega_2}(x,y) \leq u_2(x) \leq \varphi_2(y) + |||\varphi_2|||d_{\Omega_2}(x,y)$$

for all $x \in \Omega_2$, $y \in \partial\Omega_2$. It follows that

$$\varphi_2^-(x) \leq u_2(x) \leq \varphi_2^+(x).$$

The result follows as a consequence of the comparison principle stated in Theorem 2. □

Lemma 14 *Let Ω_1, Ω_2 be two open connected sets such that $\Omega_1 \cap \Omega_2 \neq \emptyset$. Let $\Omega = \Omega_1 \cup \Omega_2$. Let $\varphi_i \in Lip_\partial(\Omega_i)$, $i = 1, 2$, be such that $\varphi_1 = \varphi_2$ in $\partial\Omega_1 \cap \partial\Omega_2$. Let u_i be the $AMLE$ extension of φ_i to Ω_i. Let $\varphi \in Lip_\partial(\Omega)$ be such that $\varphi = \varphi_1$ on $\partial\Omega_1 \cap \partial\Omega$ and $\varphi = \varphi_2$ on $\partial\Omega_2 \cap \partial\Omega$. Then*

$$u_1(x) - u_2(x) \leq \sup_{\partial\Omega_1 \cap \Omega_2} (\varphi_1 - \varphi^-)^+ + \sup_{\partial\Omega_2 \cap \Omega_1} (\varphi^+ - \varphi_2)^+ \quad \textit{for all } x \in \Omega_1 \cap \Omega_2.$$

If $\partial\Omega_i \cap \Omega_j = \emptyset$, $i \neq j$, $i, j \in \{1, 2\}$, we understand that the sup value taken on it is zero.
Proof: Let u be the $AMLE$ extension of φ to Ω. By Lemma 13 we have that

$$u_i(x) - u(x) \leq \sup_{\partial\Omega_i}(\varphi_i - \varphi^-) \leq \sup_{\partial\Omega_i \cap \Omega_j} (\varphi_i - \varphi^-)^+$$

and

$$u(x) - u_i(x) \leq \sup_{\partial\Omega_i}(\varphi^+ - \varphi_i) \leq \sup_{\partial\Omega_i \cap \Omega_j} (\varphi^+ - \varphi_i)^+$$

where $j \neq i$, $i, j \in \{1, 2\}$, $x \in \Omega_i$. Hence

$$u_1(x) - u_2(x) \leq \sup_{\partial\Omega_1 \cap \Omega_2} (\varphi_1 - \varphi^-)^+ + \sup_{\partial\Omega_2 \cap \Omega_1} (\varphi^+ - \varphi_2)^+ \quad \forall x \in \Omega_1 \cap \Omega_2 \tag{11}$$

□

In next lemma we give an estimate of the error committed in the interpolated image when we have an error in the position of the level line and an error on the data given on it. The estimate on the error depends essentially on the distance between the correct and the perturbed level line and the error committed on the data.

Lemma 15 *Let Ω_i be an open bounded region contained between two curves, the exterior one J_i^+ and the interior one J_i^-, $i = 1, 2$. Assume that $J_1^- = J_2^-$. Let $\Omega = \Omega_1 \cup \Omega_2$. Let us assume that $J^- = J_1^- = J_2^-$ is the internal boundary of Ω and also that $J^+ \subseteq J_1^+ \cup J_2^+$ is the external boundary of Ω. Let φ_i be the given data on $\partial\Omega_i$ and assume that $\varphi_1 = \varphi_2$ on $\partial\Omega_1 \cap \partial\Omega_2$. Let $\varphi \in Lip_\partial(\Omega)$ be such that $\varphi = \varphi_1$ on $\partial\Omega_1 \cap \partial\Omega$ and $\varphi = \varphi_2$ on $\partial\Omega_2 \cap \partial\Omega$. Moreover, we assume that*

$$\|\varphi_2|_{J_2^+} - \lambda\|_\infty \leq \epsilon \quad \textit{and} \quad \|\varphi_1|_{J_1^+} - \lambda\|_\infty \leq \epsilon.$$

Let u_i be the $AMLE$ extension of φ_i to Ω_i. Then

$$u_1(x) - u_2(x) \leq |||\varphi||| \sup_{z \in \partial\Omega_1 \cap \Omega_2} \inf_{y \in J^+} d_\Omega(z,y) + |||\varphi||| \sup_{z \in \partial\Omega_2 \cap \Omega_1} \inf_{y \in J^+} d_\Omega(z,y) + 4\epsilon \tag{12}$$

for all $x \in \Omega_1 \cap \Omega_2$.

We have assumed for simplicity that $J_1^- = J_2^-$. A similar result can be proved when this assumption is omitted.

As above, if $\partial\Omega_i \cap \Omega_j = \emptyset$, $i \neq j$, $i, j \in \{1, 2\}$, we understand that the sup value taken on it is zero.

Proof: We shall use the estimate of Lemma 14. Observe that, if $\partial\Omega_1 \cap \Omega_2 \neq \emptyset$, we have

$$\sup_{\partial\Omega_1 \cap \Omega_2} (\varphi_1 - \varphi^-)^+ = \sup_{J_1^+ \cap \Omega_2} (\varphi_1 - \varphi^-)^+.$$

Let $x \in J_1^+ \cap \Omega_2$. Then

$$\begin{aligned} -\varphi^-(x) &= \inf_{\partial\Omega}[-\varphi(y) + |||\varphi|||d_\Omega(x,y)] \\ &\leq \inf_{J^+}[-\varphi(y) + |||\varphi|||d_\Omega(x,y)] \\ &\leq -\lambda + |||\varphi||| \inf_{J^+} d_\Omega(x,y) + \epsilon. \end{aligned}$$

Hence, if $\partial\Omega_1 \cap \Omega_2 \neq \emptyset$, we have

$$\sup_{\partial\Omega_1 \cap \Omega_2} (\varphi_1 - \varphi^-)^+ \leq |||\varphi||| \sup_{\partial\Omega_1 \cap \Omega_2} \inf_{J^+} d_\Omega(x,y) + 2\epsilon.$$

Similarly, if $\partial\Omega_2 \cap \Omega_1 \neq \emptyset$, we have

$$\sup_{\partial\Omega_2 \cap \Omega_1} (\varphi^+ - \varphi_2)^+ \leq |||\varphi||| \sup_{\partial\Omega_2 \cap \Omega_1} \inf_{J^+} d_\Omega(x,y) + 2\epsilon.$$

Adding both inequalities and using (11) we obtain (12). □

Note that we also have the estimate

$$u_1(x) - u_2(x) \leq 2|||\varphi||| \sup_{x \in J_1^+ \cup J_2^+} \inf_{y \in J^+} d_\Omega(x,y) + 4\epsilon \quad \text{for all } x \in \Omega_1 \cap \Omega_2. \tag{13}$$

Similarly we may compute the sensitivity of the interpolated image if we use a different level line and an error is committed on the data on it. The proof uses the maximum principle stated in Lemma 13 and is similar to the proof given in Lemma 15.

Lemma 16 *Let Ω_i be a bounded region contained between two curves, the exterior one J_i^+ and the interior one J_i^-, $i = 1, 2$. Assume that $\Omega_1 \subseteq \Omega_2$ and $J_1^- = J_2^-$. Let φ_i be the given data on $\partial\Omega_i$. Moreover, we assume that*

$$\|\varphi_2|_{J_2^+} - \lambda\|_\infty \leq \epsilon \quad \textit{and} \quad \|\varphi_1|_{J_1^+} - \mu\|_\infty \leq \epsilon.$$

Let u_i be the $AMLE$ extension of φ_i to Ω_i. Then

$$\sup_{\Omega_1} |u_2 - u_1| \leq |\lambda - \mu| + |||\varphi_2||| \sup_{x \in J_1^+} \inf_{y \in J_2^+} d_{\Omega_2}(x,y) + 2\epsilon \tag{14}$$

Again, we have assumed for simplicity that $J_1^- = J_2^-$, and a similar result can be proved when this assumption is omitted.

10 The coding step

We have described two algorithms that compute important points and curves from an image, thereby providing the basic geometric description of DEM data. These algorithms can be considered as a non uniform geometric sampling of the image. The next step is to interpolate the missing data from our sampling. There exists several algorithms to interpolate data from curves and/or points. We have in particular tested three of them: the Laplacian model (which corresponds to $min \int \|\nabla u\|^2$), the AMLE model (which corresponds to $min \lim_{p\to\infty} \int \|\nabla u\|^p$), and the thin plate model (which corresponds to min $\int (\triangle(u))^2$). We remark that, rigorously speaking, only the AMLE model can be used to interpolate values specified on points [3, 16, 25] (see Fig. 16). In spite of this, we shall also use the Laplacian since there are many curves in the data and we may think of points as small regions. In order to evaluate these interpolation schemes we have chosen as a measure of goodness the entropy of the residual between the original image and the interpolated one. This is a natural choice since we want to minimize the number of bits used to encode the errors between the interpolated and the original images. After several tests we have discarded the thin plate approximation since it needs to store not only the gray values at the curves but also its derivatives in order to obtain a good interpolation. The AMLE model and the simple Laplacian model were both tested using the whole image sampling (Γ_{xy} and $u|_{\Gamma_{xy}}$) and using only the level lines (Γ_M and $u|_{\Gamma_M}$). In the second case the AMLE model performed better than the Laplacian (the entropy of the residual, the maximum, and $RMSE$ errors were lower than in the Laplacian interpolation). Surprisingly, in the case of the whole sampling structure the winner was the Laplacian, although the interpolation for the AMLE model looked visually better and the maximum errors were almost the same. After these tests we have decided to use the Laplacian interpolation to obtain the first estimation of the image from the selected curves and points. In order to control the maximum (sup) error we simply store/encode the quantized error information (that is why the entropy of the residual was a natural measure of goodness for the interpolant).

At this point we need to consider how to encode both the initial curves (geometrically sampled data) and the residuals once a sup error e is specified. We proceed to address this now. The geometry of the sampled curves (Γ_{xy}) and their gray levels ($u|_{\Gamma_{xy}}$) are encoded separately. To encode the geometry we use a differential chain coding strategy, see [27, 35, 17]. Alternatively, an encoding based on rate-distortion theory, as in [54], could be used. For the gray levels, if we accept losses, we may use an ENO (Essentially Non Oscillatory) based encoding scheme [2] which also controls the sup error, a fundamental requirement of the application as stated before. Finally we compress both the geometry and the gray values of the curves using an arithmetic coder. Having these curves and the data on them, we can interpolate them by means of the Laplace equation to obtain the first estimate of the image.

Finally, to control the maximum error, we need to store the residuals r. Encoding the residuals r can be simply done by quantizing them using

$$r^q = sign(r) \left\lfloor \frac{|r|}{e} \right\rfloor e, \tag{15}$$

and then coding the resulting r^q with an arithmetic coder.

The compression ratios using this approach were already satisfactory. We observed that the encoding of the geometry represented the main cost in bits. This is due mainly to the irregularity of the curves and the inefficiency of the differential chain coding approach (3 bits/pixel with 8-connected curves or 2 bits/pixel with 4-connected curves). To further improve the encoding of the geometry we have adopted a simple multiscale approach. We compute and encode the curves and the residuals in a subsampled image and then zoom out the result and recompute new residuals. If required, before sampling, we may filter the given image with a low pass filter or with an anisotropic filter like motion by mean curvature or affine invariant smoothing [22], [53]. Indeed, it is convenient to apply these filters while keeping some points fixed, namely,

Algorithm 3

1 *From the original image, eventually filtered to reduce its bandwidth, u compute a subsampled image $u_l(i,j) = u(li, lj)$ where l is the reducing factor.*

2 *Compute Γ_{xy} and $u_l|_{\Gamma_{xy}}$. Encode Γ_{xy}. Compute $\tilde{u_l}|_{\Gamma_{xy}}$ by applying an ENO encoding scheme, with maximum error e, to $u_l|_{\Gamma_{xy}}$.*

3 *Compute the interpolated image $\tilde{u_l}$ by solving Laplace equation with initial data $(\Gamma_{xy}, \tilde{u_l}|_{\Gamma_{xy}})$.*

4 *Compute and quantize the residual r_l^q between u_l and $\tilde{u_l}$. Let $\hat{u_l} = \tilde{u_l} + r_l^q$ be the approximation of u_l satisfying $\sup\{|u_l - \hat{u_l}|\} = e$.*

5 *Zoom out $\hat{u_l}$and compute and quantize the new residual r^q between u and $\tilde{u}$ in order to satisfy $\sup\{|u - (\tilde{u} + r^q)|\} = e$.*

6 *Finally compress Γ_{xy}, $\tilde{u_l}|_{\Gamma_{xy}}$, r_l^q and r^q using an arithmetic coder.*

Table 3: Algorithm for compressing DEM data.

the points corresponding to the extrema values and the saddle points. In practice we may fix the multiple points of the sampled curves Γ_{xy}. Anisotropic filtering fixing points was studied in [11].

The zoom out process can be done by using a bicubic spline interpolation, although this can create new maxima and minima due to the well known oscillation problem of splines. In order to avoid this kind of errors we have used a *shape preserving spline*, which avoids the oscillation problem of classical splines, that is, respects the monotonicity of the original data (no new maxima or minima are created). Concretely, we have implemented the algorithm proposed in [24].

The complete algorithm for compressing DEM data is summarized in table 3.

11 Compression results

In order to compare our results, we use the JPEG-LS standard for lossless and controlled lossy image compression, being this the only standard that permits a control on the maximal per pixel error [65], and we also use JPEG-2000 [1] in which, by reintroducing the errors, we are able to control the maximum error. In the comparison tables below, JPEG-LS is denoted by JLS, while ours is denoted by ME, standing for morphological encoding. We also report the $RMSE$ as frequently done for lossy image compression algorithms. We report results on a set of 10 DEM images of size 1200 by 1200 pixels with 8 bits per pixel. We also report the results of our algorithm when applied to the same set of images with a resolution of 16 bits per pixel.

Figure 17 shows 10 plots (corresponding to a set of 10 different DEM images), each one showing the compression ratio (vertical axis) versus the maximum error allowed (horizontal axis) for both methods. When $e = 1$ there is no significant difference between both methods, though as e increases ME outperforms

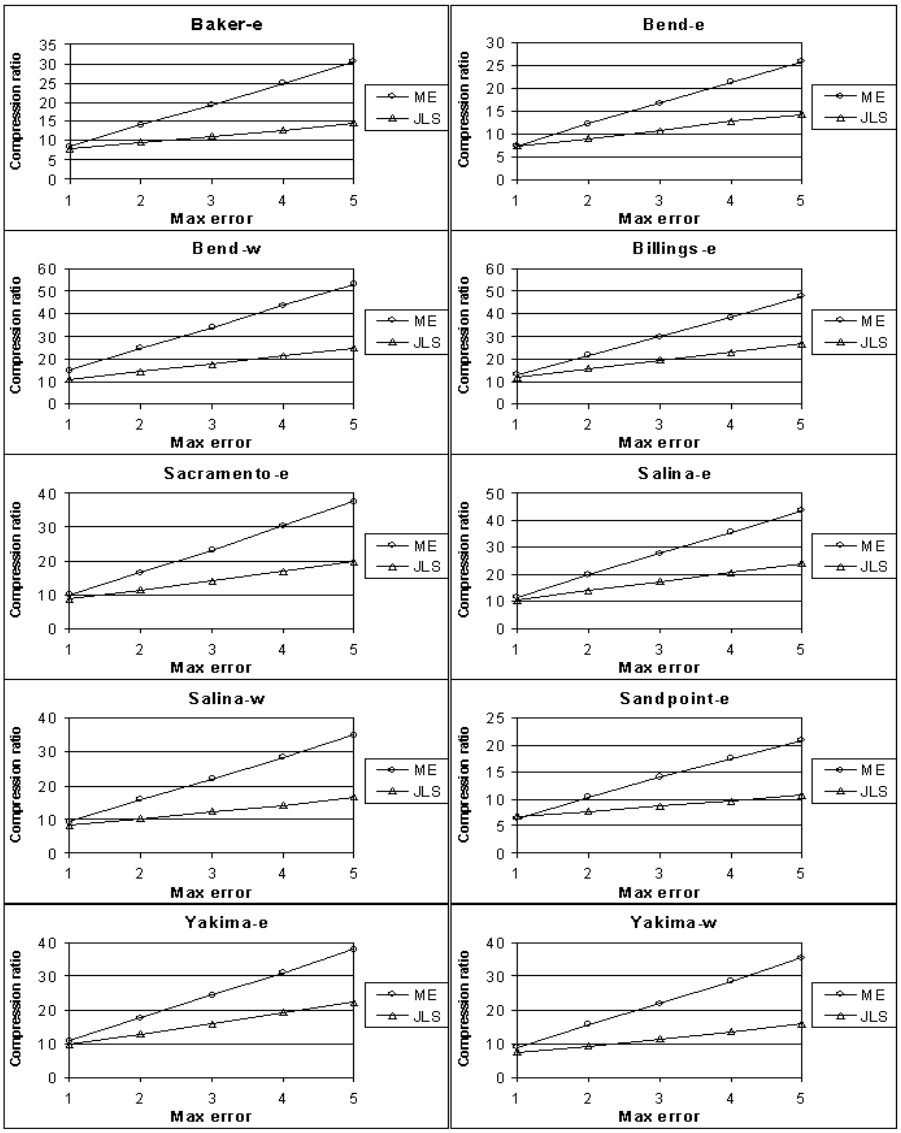

Figure 17: Performance of the compression ratio of both methods when allowing maximum errors ranging from 1 to 5. The amount in meters corresponding to a difference in gray level of 1 depends on the image, but typically this value may be of 10 meters.

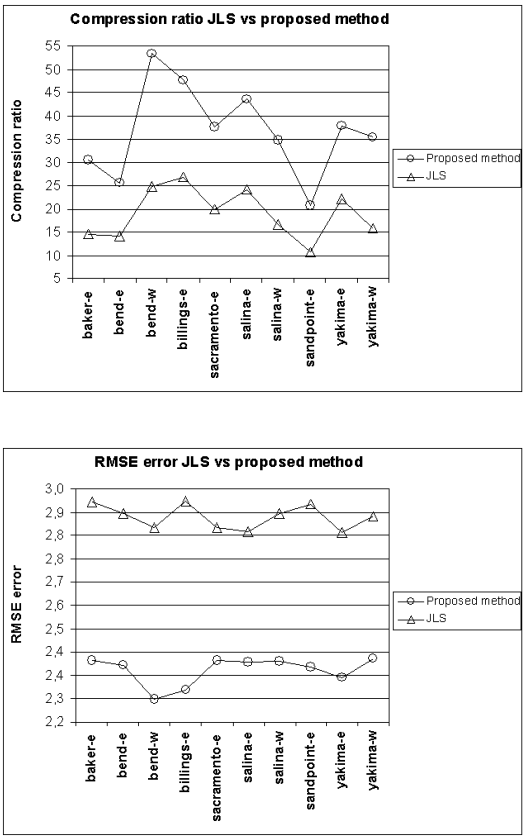

Figure 18: Top: Compression ratio of JLS vs the proposed method for a set of ten images compressed with a maximum error of 5. Bottom: Corresponding root mean square error ($RMSE$) for the two methods.

JLS. In fact when e is greater than 1 the plots show that ME reaches almost twice (or more in some cases) the compression ratio (CR) of JLS.

Figure 18 shows a more detailed study for the case $e = 5$. In the left plot we can see the compression ratio of both methods for the set of 10 images, the right plot corresponds to the $RMSE$ for both methods. Table 4 shows the exact values for the compression ratios and $RMSE$ errors of both methods. The last row shows the average values for the CR and $RMSE$ of JLS and ME. The average CR for the case of JLS and ME are **18,9872** and **36,7245** respectively. That is, our proposed scheme ME reaches almost twice the compression ratio of JLS. In addition, the average $RMSE$ for the cases of JLS and ME is **2,9038** and **2,3782**, respectively. The last two columns contain the compression ratio and the $RMSE$ in meters, respectively, corresponding to the above set of images quantized with 16 bits per pixel when compressed with ME (with $e = 5$ meters).

Table V shows the results obtained by using $JPEG - 2000$ on the above set of images. Column 1 displays the maximum error obtained when using $JPEG - 2000$ at the same compression rate as the one obtained with ME (which corresponded to a maximum error of 5) and displayed in the first column of Table IV. We also observe that we can correct the maximum error to be the same as the one obtained with ME (i.e., 5) with a negligible cost in bytes, as displayed in column 4. Column 2 contains the RMS error, which is lower than in the ME case.

Figure 19 displays the original image and its compressed versions using JLS, ME and $JPEG - 2000$.

	CR (ME) (8 bits)	CR (JLS) (8 bits)	$RMSE$ (ME)	$RMSE$ (JLS)	CR (ME) (16 bits)	RMSE (meters)
baker-e	30,4549	14,6585	2,4099	2,9546	11,1249	2,5825
bend-e	25,7138	14,2491	2,3946	2,9152	11,5988	2,5523
bend-w	53,4223	24,7324	2,2787	2,8677	15,8313	2,6217
billings-e	47,6631	26,8321	2,3121	2,9588	19,2838	2,5408
sacramento-e	37,6028	19,8254	2,4127	2,8664	9.0562	2,6763
salina-e	43,5954	24,2159	2,4062	2,8538	13,7127	2,5936
salina-w	34,8702	16,5692	2,4093	2,9166	11,5446	2,5988
sandpoint-e	20,7807	10,6721	2,3901	2,9491	9,6334	2,5501
yakima-e	37,7655	22,2050	2,3521	2,8488	17,0275	2,4659
yakima-w	35,3764	15,9119	2,4166	2,907	7,3900	2,7532
AVERAGE	**36,7245**	**18,9872**	**2,3782**	**2,9038**	**12,6203**	**2,5935**

Table 4: Columns 1 to 4: compression ratio (CR) and $RMSE$ errors for JLS and ME on 8 bit images when compressing with a maximum error of 5 gray values. Columns 5 and 6 shows the performance of the algorithm when considering the full range (16 bits), in this case the error correspond to elevation meters. The last row shows the average values for the set of 10 images.

	L_∞ no correction	$RMSE$	L_∞ corrected	increment (bytes)
baker-e	11	1,0016	5	550
bend-e	11	1,0258	5	708
bend-w	9	0,8057	5	391
billings-e	12	0,8224	5	825
sacramento-e	10	0,9689	5	568
salina-e	11	0,8961	5	615
salina-w	10	0,9635	5	630
sandpoint-e	10	1,0081	5	628
yakima-e	9	0,8748	5	504
yakima-w	9	0,9599	5	424

Table 5: First and second columns correspond to the L_∞ and $RMSE$ errors for the set of images in the first column compressed with the standard JPEG-2000 at the same compression ratio as the one achieved by our method. The third column corresponds to the L_∞ error after correcting the result achieved by JPEG-2000. The fourth column corresponds to the increment in bytes due to the correction. This increment in bytes does not affect the final compression ratio.

The figure shows both the gray scale images and its level sets. Note that the topographic structures are better preserved in the case of the ME and $JPEG-2000$ compression while it is severely distorted in the case of JLS compression.

12 Conclusions

In this work we have presented and analyzed techniques to compute a basic geometric representation of images. This representation is given by the Morse and drainage structures of the image. We have given simple algorithms to compute these structures and we have proved them to be well founded. Finally, we have proved that any interpolation process satisfying the stability and maximum principle is also shape preserving, in the sense that no new maxima or minima is created. As an application, this geometric image representation

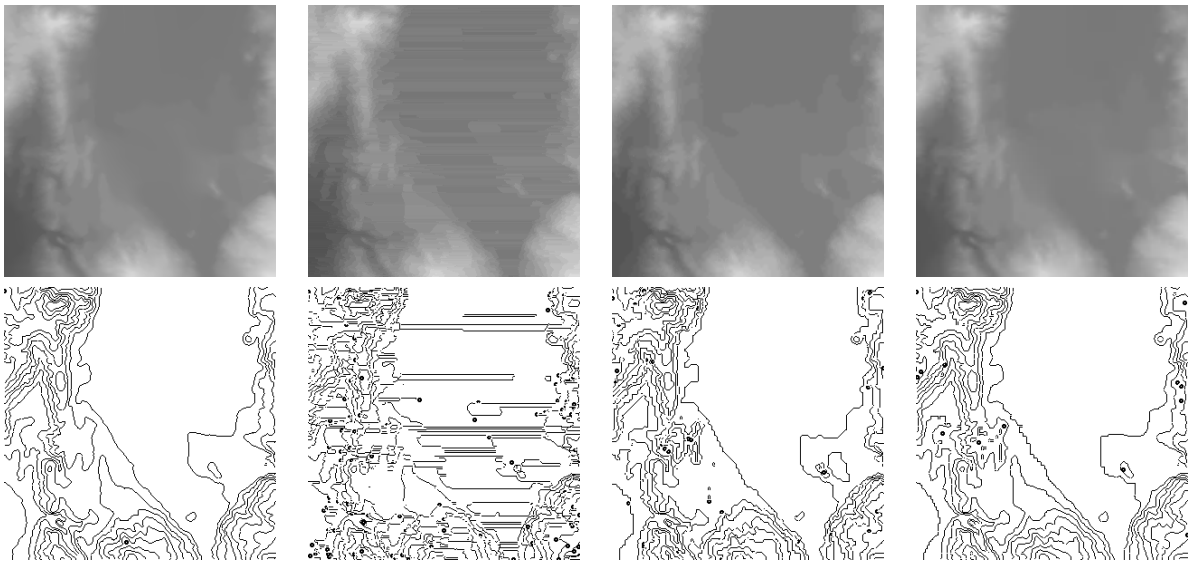

Figure 19: The first four images display the original DEM image *baker-e*, and the compressed images using JLS with sup error 5, ME with sup error 5 and $JPEG2000$ with sup error 5. Last four images: the corresponding level lines.

was used to derive a non uniform sampling strategy that when combined with interpolation and coding techniques, provided a novel DEM compression algorithm. This algorithm produces compression ratios similar to JPEG-2000 and permits to control the maximal error in the decoded image, a property which is fundamental for most DEM applications. In addition, the bit-stream encodes the most important geometric structure of DEMs, thereby providing an analysis tool and not just a compression one. We expect that the results above serve to clarify the limits of our approach.

The basic Morse and drainage structure here presented are building blocks to construct multiresolution representations of DEMs. Note that a number of criteria can be identified to provide a scoring and an order for these structures. Some of these are described for example in [7]. Level-lines and connected components can be ordered according to the area they enclose, the total gradient magnitude they represent, or any other geometric criteria. Similarly, drainage structures can be ordered according to how sharp they are (e.g., based on total curvature along them), or how long they are. This order naturally leads to multiscale representation and encoding schemes, and results in this direction will be reported elsewhere.

It would be of interest to further investigate the use of geometric sampling techniques for the compression of natural images. Some of the criteria used for the compression of DEM data, e.g., the use of an L_∞ norm, are too stringent here. Other concepts, like the selection of drainage structures, are natural for DEM data, but not as much for other types of data. The question then is what is a good geometric representation of natural images that will lead to compression results as the ones obtained for DEM with the techniques here introduced.

Acknowledgments

VC and AS acknowledge partial support by the Departament d'Universitats, Recerca i Societat de la Informació de la Generalitat de Catalunya and by PNPGC project, reference BFM2000-0962-C02-01. GS is

partially supported by a grant from the Office of Naval Research ONR-N00014-97-1-0509, the Presidential Early Career Award for Scientists and Engineers (PECASE), and a National Science Foundation CAREER Award. GS thanks Dr. Wen Masters from ONR and Dr. Carey Schwartz from DARPA for introducing him to the problem of DEM compression.

References

[1] M. D. Adams. The jpeg-2000 still image compression standard. *available at http://www.ece.ubc.ca/ mdadams*, 2001.

[2] F. Aràndiga and R. Donat. Nonlinear multiscale decompositions: The approach of A. Harten. *Numerical Algorithms*, 23:175–216, 2000.

[3] G. Aronssson. Extension of functions satisfying lipschitz conditions. *Ark. for Math.*, 6:551–561, 1967.

[4] G. Aronssson. On the partial differential equation $u_x^2 u_{xx} + 2u_x u_y u_{xy} + u_y^2 u_{yy} = 0$. *Ark. for Math.*, 7:395–425, 1968.

[5] G. Aronssson. On certain singular solutions of the partial differential equation $u_x^2 u_{xx} + 2u_x u_y u_{xy} + u_y^2 u_{yy} = 0$. *Manuscripta Mathematica*, 47:133–151, 1984.

[6] C. Bajaj, V. Pascucci, and D.R. Schikore. Fast isocontouring for improved interactivity. *In Proc. IEEE Symposium on Volume Visualization, San Francisco, Oct. 7-8*, pages 39–46, 1996.

[7] C. Bajaj, V. Pascucci, and D.R. Schikore. The contour spectrum. *Proceedings Visualization '97*, pages 167–173, 1997.

[8] C. Ballester and V. Caselles. The m-components of level sets of continuous functions in wbv. *Publicacions Matemàtiques*, 45:477–527, 2001.

[9] C. Ballester, V. Caselles, and P. Monasse. The tree of shapes of an image. *To appear in ESAIM: COCV*, 2002.

[10] P.J. Besl and R.C. Jain. Segmentation through symbolic surface descriptions. *CVPR, May*, 1986.

[11] V. Caselles, B. Coll, and J.M. Morel. A kanizsa programme. *Progress in Nonlinear Diferential Equations and their Applications*, 25, 1996.

[12] V. Caselles, B. Coll, and J.M. Morel. Topographic maps and local contrast changes in natural images. *Int. J. Comp. Vision*, 33(1):5–27, 1999.

[13] V. Caselles, J. L. Lisani, J.M. Morel, and G. Sapiro. Shape preserving local histogram modification. *IEEE Transactions on Image Processing*, 8(2):220–230, 1999.

[14] V. Caselles and P. Monasse. Grain filters. *to appear in Journal of Mathematical Imaging and Vision*, 2002.

[15] V. Caselles, P. Monasse, and A. Solé. Morse descriptions of the topographic map of an image. *In preparation*, 2002.

[16] V. Caselles, J.M. Morel, and C. Sbert. An axiomatic approach to image interpolation. *IEEE Transactions on Image Processing, Special Issue on PDE's, Geometry Driven Diffusion and Image Processing*, 7(3):376–386, 1998.

[17] B. B. Chaudhuri and S. Chandrashekhar. Neighboring direction runlength coding: An efficient contour coding scheme. *IEEE Transactions on Systems, Man and Cybernetics*, 20(4):916–921, July 1990.

[18] J.L. Cox and D.B. Karron. Digital morse theory with suggested applications. *Manuscript available at http://www.casi.net*, 1998.

[19] A. Desolneux, L. Moisan, and J.M. Morel. Edge detection by helmholtz principle. *To appear at the Journal of Mathematical Imaging and Vision*, 2001.

[20] W.R. Franklin and A. Said. Lossy compression of elevation data. *7th Int. Symposium on Spatial Data Handling*, 1996.

[21] J. Froment. A functional analysis model for natural images permitting structured compression. *COCV*, 4:473–495, 1999.

[22] F. Guichard and J.M. Morel. Partial differential equations and image iterative filtering. *Ceremade, 9535, Université Paris-Dauphine, France*, 1995.

[23] R. Haralick, L. Winston, and T. Laffey. The topographic primal sketch. *Int. J. Rob. Research*, 2, 1983.

[24] J. M. Hyman. Monotonicity preserving cubic interpolation. *SIAM J. Sci. Stat. Comp.*, 4(4), 1983.

[25] R. Jensen. Uniqueness of lipschitz extensions: Minimizing the sup norm of the gradient. *Arch. Rat. Mech. Anal.*, 123:51–74, 1993.

[26] E.G. Johnston and A. Rosenfeld. Digital detection of pits, peaks, ridges and ravines. *IEEE Trans. Systems Man Cybernetics*, 472(July), 1975.

[27] R. R. Estes Jr. and V. Ralph Algazi. Efficient error free chain coding of binary documents. *Proceedings of the Data Compression Conference, Snowbird, Utah*, pages 122–132, April 1995.

[28] A.S. Kronrod. On functions of two variables. *Uspehi Mathematical Sciences (NS)*, 35(5):24–134, 1950.

[29] C. Kuratowski. Topologie i, ii. *Editions J. Gabay*, 1992.

[30] I.S. Kweon and T. Kanade. Extracting topograpic terrain features from elevation maps. *CVGIP: Image Understanding*, 59(2):171–182, 1994.

[31] C. Lantuéjoul and S. Beucher. On the use of geodesic metric in image analysis. *J. Microscopy*, 121:39–49, 1981.

[32] C. Lantuéjoul and F. Maisonneuve. Geodesic methods in image analysis. *Pattern Recognition*, 17:117–187, 1984.

[33] J.L. Lisani. Comparaison automatique d'images par leurs formes. *Ph.D Thesis, Université de Paris-Dauphine, July*, 2001.

[34] A. López, F. Lumbreras, J. Serrat, and J. Villanueva. Evaluation of methods for ridge and valley detection. *IEEE Trans. on Pattern Analysis and Machine Intelligence*, 21(4), 1999.

[35] C. Lu and J. Dunham. Highly efficient coding schemes for contour lines based on chain code representation. *IEEE Trans. Commun.*, 39(10):1511–1514, 1991.

[36] F. Meyer and S. Beucher. Morphological segmentation. *J. Visual Commun. Image Representation*, 1:21–46, 1990.

[37] J. Milnor. Morse theory. *Annals of Math. Studies 51, Princeton University Press*, 1963.

[38] P. Monasse. *Représentation morphologique d'images numériques et application au recalage*. PhD thesis, Université de Paris-Dauphine, 2000.

[39] P. Monasse and F. Guichard. Fast computation of a contrast invariant image representation. *IEEE Trans. on Image Proc.*, 9:860–872, 2000.

[40] M.H.A. Newman. Elements of the topology of plane sets of points. *Dover Publications, New York*, 1992.

[41] F. Meyer P. Salembier, L. Torres and C. Gu. Region-based video coding using mathematical morphology. *Proceedings of IEEE (Invited paper)*, 83(6):843–857, 1995.

[42] L. Garrido P. Salembier. Binary partition tree as an efficient representation for image processing, segmentation, and information retrieval. *IEEE Transactions on Image Processing*, 9(4):561–576, 2000.

[43] S.D. Rane and G. Sapiro. Evaluation of JPEG-LS, the new lossless and controlled-lossy still image compression standard, for compression of high-resolution elevation data. *IEEE Transactions on Geoscience and Remote Sensing*, 39(10):2298–2306, October 2001.

[44] G. Reeb. Sur les poits singuliers d'une forme de pfaff completement integrable ou d'une fonction numérique. *Comptes Rendus Acad. Sciences Paris*, 222:847–849, 1946.

[45] E. Reusens. Joint optimization of representation model and frame segmentation for generic video compression. *EURASIP Signal Processing*, 46(11):105–117, 1995.

[46] E. Rosset. A lower bound for the gradient of ∞-harmonic functions. *Electronic J. of Diff. Equations*, pages 1–7, 1996.

[47] J. Roubal and T.K. Poiker. Automated contour labelling and the contour tree. *In Auto-Carto, March*, 1985.

[48] A. Said and W. A. Pearlman. An image multiresolution representation for lossless and lossy comression. *IEEE Transaction on Image Processing*, 5(9):1303–1310, September 1996.

[49] P. Salembier. Morphological multiscale segmentation for image coding. *Signal Processing, Special Issue on Nonlinear Signal Processing*, 38:359–386, 1994.

[50] P. Salembier, P. Brigger, J.R. Casas, and M. Pardàs. Morphological operators for image and video compression. *IEEE Trans. on Image Processing*, 5:881–897, 1996.

[51] P. Salembier and F. Marqus. Region-based representations of image and video: Segmentation tools for multimedia services. *IEEE Transactions on Circuits and Systems for Video Technology*, 9(8):1147–1169, 1999.

[52] P. Salembier and J. Serra. Flat zones filtering, connected operators and filters by reconstruction. *IEEE Trans. Image Processing*, 4:1153–1160, 1995.

[53] G. Sapiro and A. Tannenbaum. Affine invariant scale-space. *International Journal of Computer Vision*, 11:25–44, 1993.

[54] G.M. Schuster and A.K. Katsaggelos. *Rate-distortion based video compression.* Kluwer Academic Publishers, 1997.

[55] W.W. Seemuller. The extraction of ordered vector drainage networks from elevation data. *Comp. Vision Graphics and Image Processing,* 47, 1989.

[56] J. Serra and P. Salembier. Connected operators and pyramids. *Proc. SPIE Image Algebra Math. Morphology, San Diego, CA, SPIE*, 2030:65–76, 1993.

[57] Y. Shinagawa, T.L. Kunii, and Y.L. Kergosien. Surface coding based on morse theory. *IEEE Computer Graphics and Appl.*, 11(5):66–78, 1991.

[58] A. Solé, V. Caselles, G. Sapiro, and F. Arándiga. Morse description and geometric encoding of digital elevation maps. *IMA Technical report (www.ima.umn.edu)*, 2002.

[59] S.M. Srivastava. *A Course on Borel Sets.* Springer Verlag, San Diego, 1998.

[60] S. Takahashi, T. Ikeda, Y. Shinagawa, T. Kunii, and M. Ueda. Algorithms for extracting correct critical points and constructing topological graphs from discrete geographic elevation data. *Eurographics 95*, 14(3):181–192, 1995.

[61] M. van Kreveld, R. va Oostrum, C. Bajaj, V. Pascucci, and D. Schikore. Contour trees and small seed sets for isosurface traversal. *In 13th ACM Symposium on Computational Geometry*, pages 212–220, 1997.

[62] L. Vincent. Gray scale area openings and closings, their efficient implementation and applications. *Proc. Workshop Mathematical Morphology and Applications to Signal Processing, Barcelona, Spain, May*, pages 22–27, 1993.

[63] L. Vincent. Morphological area openings and closings for gray-scale images. *Proc. of the Workshop "Shape in Picture",1992, Driebergen, The Netherlands, Springer-Berlin*, pages 197–208, 1994.

[64] L. Vincent and P. Soille. Watersheds in digital spaces: An efficient algorithm based ion immersion simulations. *IEEE Trans. Pattern Anal. Machine Intell.*, 13:583–598, 1991.

[65] M.J. Weinberger, G. Seroussi, and G. Sapiro. From LOCO-I to the JPEG-LS standard. *Proceedings of the International Conference on Image Processing*, 4:68–72, 1999.

[66] M.J. Weinberger, G. Seroussi, and G. Sapiro. LOCO-I: A low complexity, context-based, lossless image compression algorithm. *Proc. IEEE Data Compression Conf., Snowbird, Utah*, April, 1996.